Response to Reviewer 1

1 Overall assessment

Reviewer — The manuscript uses 9 years of CALIPSO level 3 gridded monthly data to separate the tropical cirrus clouds into those from convective and non-convective origin. The authors define clouds associated with positive specific humidity anomalies as convective origin and clouds associated with negative temperature anomalies as non-convective origin cirrus. While their method seems overly simplistic at first sight, their robust, physically justifiable results speak for themselves and helped overcome my initial skepticism about the use of very coarse time and spatial resolution of the satellite dataset. This is a nice and clear study, and I recommend publication after the listed comments are addressed.

Authors — We thank the reviewer for his encouraging feedback and for the helpful questions and comments below. Prompted by the feedback from both reviewers, we have made changes to the manuscript and believe it has been significantly improved as a result. The list of major changes to the manuscript is attached. It may be helpful for the readers to refer to the list of changes before reading the discussions below. We are also attaching two versions of the revised manuscript, one with tracked changes and one without tracked changes. The discussions below refer to the line numbers in the version with tracked changes. Please find below our point-by-point reply, first to the general comments, followed by the minor comments of the reviewer.

2 General comments

1. ***Reviewer*** — With CALIPSO, you are limited to clouds with optical thickness smaller than about 3. Is this a significant limitation of the study? What proportion of the clouds is missed?

   Authors — We are indeed limited to clouds with optical depths (ODs) smaller than about 3 with CALIPSO. This is not a significant limitation of the study because only a small or negligible number of clouds are missed as there are few cirrus clouds with ODs greater than 3. CALIPSO user guide shows that cirrus cloud frequency decreases exponentially with increasing OD for OD larger than 0.2 and that more than 90 % of cirrus clouds have ODs less than 1 (see `https://www-calipso.larc.nasa.gov/resources/calipso_users_guide/data_summaries/profile_data.php`). Other independent measurements also confirm that the majority of cirrus clouds are optically thin with ODs less than 3. For example, ground-based lidar measurements showed that, over the tropical Amazonia region, cirrus clouds with ODs less than

0.3 account for about 80 % of all cirrus clouds; the remaining 20 % are cirrus with ODs greater than 0.3 (Gouveia et al., 2017). In another study by Kumar and Venkatramanan (2020) using a ground-based Mie lidar, cirrus clouds with ODs greater than 0.3 were found to account for only 14 % of cirrus clouds observed over Gadanki, India. From these numbers and the exponential decrease of cirrus cloud frequency with increasing OD, we estimate that cirrus clouds with ODs greater than 0.3 account for about 10–20 % of tropical cirrus clouds, and cirrus clouds with ODs greater than 3 probably account for less than a few percent of tropical cirrus clouds.

2. ***Reviewer*** — Is it fair to say that a positive specific humidity anomaly must be associated with convection? What if convection with relative humidity with respect to ice of 100 % reaches an ice supersaturated region? There is ample evidence that deep convection on average hydrates the upper troposphere, but I think the authors should nevertheless discuss the other possibility and how it could influence their results.

   Authors — It is true that some convection events can produce negative specific humidity (SPH) anomaly. For this reason and the reasons pointed out by the second reviewer, we have changed the terminology used in the manuscript, from cirrus that originate from convection and non-convective processes to moist and dry cirrus, respectively. The new names refer to how we classify the clouds based on the SPH and temperature anomalies. We no longer assume a priori that convection always leads to hydration. The new terminology does not change the main results of the analysis, i.e., that the monthly spatiotemporal distribution of moist cirrus (formerly convective cirrus) is consistent with that of convection, while the monthly spatiotemporal distribution of dry cirrus (formerly non-convective cirrus) is distinct from that of convection. The latter result indicates that convection events that lead to negative SPH anomaly do not happen frequently enough to show up in the monthly data. The monthly seasonal patterns of both high-altitude dry cirrus (Fig. 8b) and low-altitude dry cirrus (Fig. 8d) are distinct from that of convection. In other words, on the monthly and seasonal time scales, the population of dry cirrus is not driven by convection.

3. ***Reviewer*** — Could you verify your cloud classification method on a subset of instantaneous CALIPSO profile data? Would the results based on instantaneous data agree with the gridded, 1-monthly data?

   Authors — We have verified the method with the CALIPSO Level 2 cloud profile dataset v4.20 (`https://asdc.larc.nasa.gov/project/CALIPSO/CAL_LID_L2_05kmCPro-Standard-V4-20_V4-20`) for January 2015. The time resolution of the CALIPSO Level 2 data is 0.74 s. Due to limited computer resources, we cannot process the data at this resolution. Therefore, we averaged the Level 2 data over time to obtain the daily data for January 2015. The daily meteorological conditions were obtained from ERA5 for the same month and used for the classification of clouds in the daily-averaged Level 2 data. Figure 1 shows that the occurrence of moist and dry cirrus is qualitatively consistent between CALIPSO Level 2 and Level 3 datasets.

3 Specific comments

1. ***Reviewer*** — Abstract: For clarity, I suggest avoiding the use of abbreviations in the abstract (unless strictly needed).

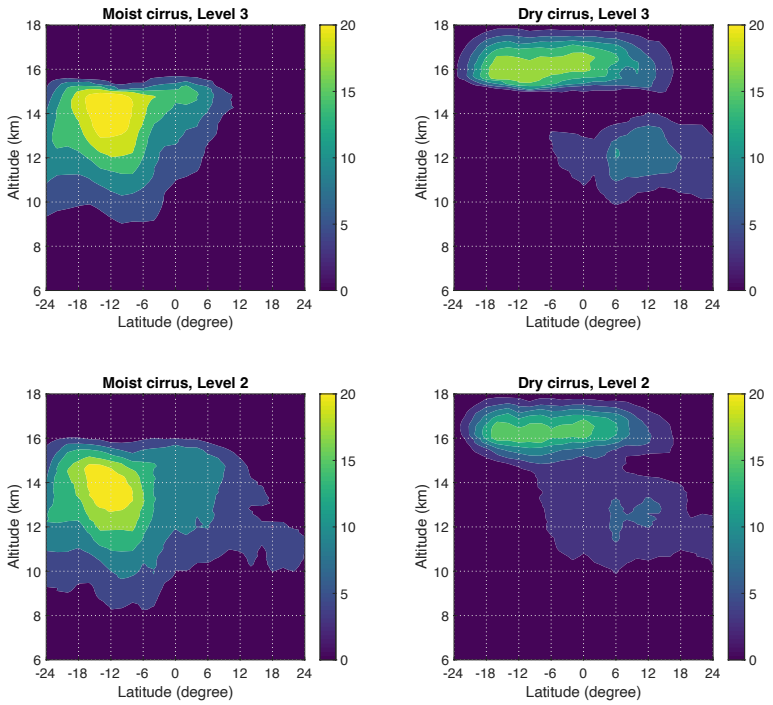

Figure 1: Latitude–altitude profiles of the frequency of occurrence of moist cirrus (left) and dry cirrus (right) in January 2015, derived from CALIPSO Level 3 Ice Cloud Product (top) and CALIPSO Level 2 Ice Cloud Product (bottom).

Authors — We agree and have removed all abbreviations from the abstract.

2. ***Reviewer*** — Introduction: I'm missing a few more lines describing why it is important to separate the origin of cirrus. In principle, the models could simulate the correct cloud amount and cirrus properties even without correctly accounting for their origin.

   Authors — We have revised the introduction to discuss that our motivation is the occurrence of cirrus clouds in response to the SPH and temperature anomalies. The origins of cirrus clouds are inferred from the corresponding analysis for academic interests, while the analysis of cloud occurrence in response to the SPH and temperature anomalies has practical modeling applications. The sentence "The purpose of this paper is to quantify the roles of convection and non-convective processes in governing the occurrence of cirrus clouds." has been removed (please see lines 33–34). To clarify the applications in modeling practice, we added the following text to the end of the manuscript (lines 407–414):

   "The method proposed here to study cirrus clouds can be applied in model development to improve the representation of cirrus clouds in numerical simulations. We have demonstrated that the spatiotemporal distribution of cirrus clouds is governed by the SPH, temperature, and their variations. Therefore, models would need to accurately represent the SPH, temperature, and their variances in order to accurately simulate the distribution of cirrus clouds. It would be useful to compare between observations and numerical simulations in terms of the frequency and magnitude of the moisture and temperature anomalies and how they affect the occurrence of cirrus clouds. Such a comparison would reveal the specific strategies on how to adjust the model parameterization schemes (e.g., the convection scheme, the gravity wave drag scheme, and/or the microphysics scheme) to improve the representation of cirrus clouds in models."

3. ***Reviewer*** — Line 26: Li et al., 2012 (doi: 10.1029/2012JD017640) may be a good reference about the uncertainties in cirrus, at least with respect to the ice water content.

   Authors — Li et al. (2012) is now cited on line 32.

4. ***Reviewer*** — Lines 46–47: The sentence starting with "Wang and Dessler" is missing something.

   Authors — We added "For example, " before Wang and Dessler (2012) on line 52.

5. ***Reviewer*** — Line 48: It may be appropriate to add references explicitly looking at the decay of convective origin clouds. If I am not mistaken, the cited papers all refer to the evolution of in-situ TTL cirrus.

   Authors — Thank you for letting us know about these relevant papers. The papers by Gehlot and Quaas (2012) and Gasparini et al. (2021) on the decay of convective-origin cirrus clouds are now cited on lines 56–57 and 405–406.

6. ***Reviewer*** — Lines 59–62: I would suggest also mentioning studies using high cloud trajectories in climate models, e.g., Gehlot and Quaas, 2012 (doi: 0.1175/JCLI-D-11-00345.1) and Gasparini et al., 2021 (doi: 10.1175/JCLI-D-11-00345.1).

   Authors — Here we discuss how Lagrangian trajectory calculations were used to distinguish cirrus of convective and non-convective origins. On the other hand, Gehlot and Quaas (2012) and Gasparini et al. (2021) focused on convective-origin cirrus clouds only. Therefore, we reference

these two papers elsewhere (lines 56–57 and 405–406). The paper by Luo and Rossow (2004) which was cited here originally has also been moved to lines 56–57 and 405–406 where processes that affect the decay of cirrus clouds are discussed.

7. ***Reviewer*** — Lines 90–92: Does your method work also for regions with a limited annual cycle of convection, e.g., for parts of the tropical western Pacific?

   Authors — Yes, our method works there.

8. ***Reviewer*** — Section 3: How is cloud fraction defined? Can it be only 0 or 1 or is it also expressed as a fraction? If fractions are used, how do you consider them in the analysis of in-cloud vs clear-sky grid boxes?

   Authors — The ice cloud fraction (ICF) is calculated by,

$$\mathrm{ICF} = \frac{ice\_cloud\_accepted\_samples}{cloud\_accepted\_samples + cloud\_rejected\_samples + cloud\_free\_samples},$$

   (see `https://www-calipso.larc.nasa.gov/resources/calipso_users_guide/qs/cal_lid_l3_cloud_occurrence_v1-00.php`). The ICF varies between 0 and 1. At a given time, a grid box is considered cloudy if the ICF is greater than 0.01. We have added the definition of cloudy grid boxes to lines 140–142.

9. ***Reviewer*** — Figure 3: I would suggest using a symlog scaling (`https://matplotlib.org/stable/gallery/scales/symlog_demo.html`), so that one can see more than just the temperature-dependent increase in Dq (i.e., basically Clausius–Clapeyron). If you use matplotlib for plotting, this is how you could do it: plt.gca().set–yscale('symlog', linthreshy=1e-2).

   Authors — Thanks for this suggestion. The figure is now plotted in logarithmic scale.

10. ***Reviewer*** — Figure 5: density = IWC, right? Please, be consistent. Caveat: CALIPSO lidar will not penetrate into optically thick clouds, so the lower part of the plot is biased to low IWC.

    Authors — We have changed the word 'density' into 'IWC' for consistency in the revised manuscript. Although CALIPSO retrieval of IWC may not be perfect, it was found to be in good agreement with the radar-lidar retrieval over Darwin, Australia (Protat et al., 2010).

11. ***Reviewer*** — Lines 209–218: Please, don't use parentheses to indicate the opposite of an idea. This makes the text really hard to understand. See also `https://eos.org/opinions/parentheses-are-are-not-for-references-and-clarification-saving-space`.

    Authors — We have rewritten these so that parentheses are no longer used. Please see lines 281–289.

12. ***Reviewer*** — Figure 10: Could you explicitly mention already in the caption that you show an "all-sky" average?

    Authors — Figure 10 now shows the profiles of both the grid-average IWC and in-cloud IWC. The caption refers to the "grid-average" (instead of "all-sky") IWC so as to be consistent with CALIPSO terminology (see `https://www-calipso.larc.nasa.gov/resources/calipso_users_guide/qs/cal_lid_l3_ice_cloud_v1-00.php`).

13. ***Reviewer*** — Line 263: It's really hard to see from Fig. 9 if the average/median IWC of convective and non-convective cirrus are comparable in a given temperature bin or not. Could you for example express it in numbers/median values? Also, the IWC is certainly biased low at $T > 240\,\mathrm{K}$ due to the limitations of the CALIPSO lidar measurements.

    Authors — We added the vertical profiles of the in-cloud IWC in moist and dry cirrus to Fig. 10. These profiles show more clearly (than Fig. 9) that the average IWCs in moist and dry cirrus are comparable. The biases in IWCs would affect moist and dry cirrus equally and so they would not alter our conclusion that the IWCs moist and dry cirrus are comparable for a given temperature/altitude bin.

14. ***Reviewer*** — Line 303: As in the introduction, it may be worthwhile to add some citations that actually studied the decay of convective-origin cirrus, and not only the in-situ generated cirrus.

    Authors — We now cite Gehlot and Quaas (2012) and Gasparini et al. (2021) here. Please see line 405–406.

References

B. Gasparini, P. J. Rasch, D. L. Hartmann, C. J. Wall, and M. Dütsch. A Lagrangian Perspective on Tropical Anvil Cloud Lifecycle in Present and Future Climate. *J. Geophys. Res. Atmos.*, 126 (4):e2020JD033487, 2021. doi: 10.1029/2020JD033487.

S. Gehlot and J. Quaas. Convection–Climate Feedbacks in the ECHAM5 General Circulation Model: Evaluation of Cirrus Cloud Life Cycles with ISCCP Satellite Data from a Lagrangian Trajectory Perspective. *J. Climate*, 25(15):5241–5259, 2012. doi: 10.1175/JCLI-D-11-00345.1.

D. A. Gouveia, B. Barja, H. M. J. Barbosa, P. Seifert, H. Baars, T. Pauliquevis, and P. Artaxo. Optical and geometrical properties of cirrus clouds in Amazonia derived from 1 year of ground-based lidar measurements. *Atmos. Chem. Phys.*, 17(5):3619–3636, 2017. doi: 10.5194/acp-17-3619-2017.

N. M. Kumar and K. Venkatramanan. Lidar Observed Optical Properties of Tropical Cirrus Clouds Over Gadanki Region. *Front. Earth. Sci.*, 8, 2020. doi: 10.3389/feart.2020.00140.

J.-L. F. Li, D. E. Waliser, W.-T. Chen, B. Guan, T. Kubar, G. Stephens, H.-Y. Ma, M. Deng, L. Donner, C. Seman, and L. Horowitz. An observationally based evaluation of cloud ice water in CMIP3 and CMIP5 GCMs and contemporary reanalyses using contemporary satellite data. *J. Geophys. Res.*, 117(D16):D16105, 2012. doi: 10.1029/2012JD017640.

Z. Luo and W. B. Rossow. Characterizing Tropical Cirrus Life Cycle, Evolution, and Interaction with Upper-Tropospheric Water Vapor Using Lagrangian Trajectory Analysis of Satellite Observations. *J. Climate*, 17(23):4541–4563, 2004.

A. Protat, J. Delanoë, E. J. O'Connor, and T. S. L'Ecuyer. The Evaluation of CloudSat and CALIPSO Ice Microphysical Products Using Ground-Based Cloud Radar and Lidar Observations. *J. Atmos. Ocean. Technol.*, 27(5):793–810, 2010. doi: 10.1175/2009JTECHA1397.1.

T. Wang and A. E. Dessler. Analysis of cirrus in the tropical tropopause layer from CALIPSO and MLS data: A water perspective. *J. Geophys. Res.*, 117:D04211, 2012. doi: 10.1029/2011JD016442.

List of major changes

This document lists the major changes that have been made in the revised manuscript.

1. We have changed the terminology used in the manuscript, from cirrus that originate from convection and non-convective processes to moist and dry cirrus, respectively. Moist cirrus are the clouds in which there are positive specific humidity anomalies, and dry cirrus are those in which there are negative specific humidity anomalies and negative temperature anomalies. The new terminology does not change the main results of the analysis, i.e., that the monthly spatiotemporal distribution of moist cirrus (formerly convective cirrus) is consistent with that of convection, while the monthly spatiotemporal distribution of dry cirrus (formerly non-convective cirrus) is distinct from that of convection. Because of the change in the terminology, the title of the manuscript also needs to be changed. The old title is "Tropical cirrus clouds of convective and non-convective origins", and the new title is "Monthly occurrence of tropical cirrus clouds explained by monthly moisture and temperature variations".

2. We have revised our method (please see Section 3 in the manuscript) to use the all-sky condition as the background state in the definitions of the specific humidity (SPH) and temperature anomalies between cloud samples and the background state. The cloud-free condition was used originally. This change improves the method because the all-sky condition is more representative of the mean background state than the cloud-free condition. In particular, the SPH anomaly between the cloud sample at the location (x,y,z) and time t and the background state is defined as $\Delta q(x,y,z,t) = q_{\rm cld}(x,y,z,t) - \overline{q}(x,y,z)$. The time-average SPH ($\overline{q}$) is obtained by averaging the SPH over all the times in the dataset regardless of whether clouds are present in the grid box. Similarly, $\Delta T(x,y,z,t) = T_{\rm cld}(x,y,z,t) - \overline{T}(x,y,z)$ is the difference between the temperature in the cloud sample at the location (x,y,z) and time t and the time-average temperature at the same location. The revision of the method does not change our conclusions qualitatively and the behaviours of moist and dry cirrus are qualitatively similar to those of convective and non-convective cirrus in the original manuscript. However, the percentage contributions of the two categories of clouds have changed quantitatively and the numbers in Table 2 are different from before.

3. Figure 5 has been replaced by a new figure. Figures 5(c) and 5(d) in the original manuscript show the latitude–altitude profiles of the grid-average ice water content (IWC) of cirrus clouds. The latitudinal profile of the IWC can be inferred from the latitudinal profile of the ice water path (IWP) shown in Fig. 8 and the vertical profile of the grid-average IWC is now shown in Fig. 10. Therefore, we decided to delete Figs. 5(c) and 5(d) as the information

in these panels is now redundant. The original Figs. 5(a) and 5(b) are combined into the new Fig. 5(a). The new Fig. 5(b) shows the vertical profile of the climatological mean frequency of occurrence of cirrus clouds separately for the Northern Hemisphere and Southern Hemisphere.

4. Figure 6 has been replaced by a new figure. In the original manuscript, Fig. 6(a) shows the latitudinal profile of the vertical maximum of the climatological zonal mean frequency of occurrence of cirrus clouds and Fig. 6(b) shows the monthly variations of the tropical mean vertical maximum frequency of occurrence of cirrus clouds. We removed the original Fig. 6(a) since the latitudinal profile of the climatological mean frequency of occurrence of cirrus clouds has been shown in Fig. 5(a). We removed the original Fig. 6(b) since the monthly variations of the vertical maximum frequency of occurrence of cirrus clouds has been shown in Fig. 8. The new Fig. 6 shows the latitude–altitude profile of the frequency of occcurrence of cirrus clouds in the four seasons.

Monthly occurrence of tropical cirrus clouds explained by monthly moisture and temperature variations

Qin Huang[1] and Tra Dinh[1]

[1]Department of Physics, University of Auckland, Auckland, New Zealand

Correspondence: Tra Dinh (t.dinh@auckland.ac.nz)

Abstract. The occurrence of cirrus clouds in the tropics (24 °S–24 °N) is analyzed using the 2007–2015 monthly data from the Cloud-Aerosol Lidar and Infrared Pathfinder Satellite Observation ~~(CALIPSO)~~ and the fifth generation reanalysis product ~~(ERA5)~~ of the European Centre for Medium-Range Weather Forecasts. ~~In most cirrus clouds,~~ The data show that the specific humidity ~~(SPH) is larger than in cloud-free air~~ is larger and/or the temperature is smaller ~~than in cloud-free air~~in most cirrus clouds than in the average all-sky condition at the same location. Both positive ~~SPH perturbations~~ specific humidity anomalies and negative temperature ~~perturbations~~ anomalies increase the relative humidity, resulting in favorable conditions for the formation and maintenance of clouds. ~~The~~ We refer to the clouds in which there are positive ~~SPH perturbations are considered to originate from convection. This is because, in~~ specific humidity anomalies as moist cirrus, and those in which there are negative specific humidity anomalies and negative temperature anomalies as dry cirrus. In the free troposphere, positive ~~SPH~~ specific humidity anomalies are largely produced by the upward transport of moisture by convection followed by detrainment of the convective plumes. ~~The remaining clouds that are not directly~~ Therefore, moist cirrus are strongly influenced by convection~~are driven by negative temperature perturbations. These temperature-driven clouds~~ . On the other hand, dry cirrus are formed and maintained in the cold phases of gravity waves and/or by the adiabatic cooling associated with the upwelling branch of the Brewer–Dobson circulation. Averaged over all altitudes of the tropical atmosphere, ~~there are about three times more convective cirrusthan non-convective ones~~moist cirrus are about twice as abundant as dry cirrus. The level of maximum ~~convective cirrus occurrence is at~~ occurrence of moist cirrus is near 14 km, i.e., the bottom of the tropical tropopause layer~~(TTL). Non-convective~~ . Dry cirrus obtain their maximum frequency of occurrence at about 16 km, which is below the cold point tropopause~~(CPT)~~. The seasonal cycle of ~~convective cirrus is~~ moist cirrus is found to be consistent with that of tropical convection, while the seasonal cycle of ~~non-convective~~ dry cirrus in the ~~TTL~~ tropical tropopause layer is consistent with that of the ~~CPT~~cold point tropopause. There are two maxima in the frequency of occurrence of ~~convective~~ moist cirrus, one at around ~~10 °S~~ 11 °S–12 °S in the austral summer, and the other at around ~~10 °N~~ 11 °N–12 °N in the boreal summer. In contrast, ~~non-convective~~ dry cirrus occur most frequently near the equator in the boreal winter. The ice water content ~~(IWC) in both convective and non-convective~~ in both moist and dry cirrus increases with increasing temperature (decreasing altitude). Thus, ~~non-convective~~ dry cirrus—which on average occur at lower temperatures (higher altitudes)—tend to have lower ~~IWCs than convective~~ ice water contents than moist cirrus.

1 Introduction

Cirrus are ice clouds which are typically found in the cold atmosphere above 6 km–8 km. Cirrus clouds occur as frequently as 20 % to 70 % of the time over the different regions of the globe [*Wang et al.*, 1996; *Mace et al.*, 2009; *Hong and Liu*, 2015; *Heymsfield et al.*, 2017]. Their radiative effects ~~significantly~~ influence the dynamics and thermodynamics of the atmosphere [*Liou*, 1986]. ~~To date, the roles of the different processes that govern the occurrence of cirrus clouds remain not well quantified. This contributes to uncertainties~~ However, large uncertainties exist in estimating cirrus cloud amount and their spatiotemporal distribution and radiative effects in contemporary models [see e.g. *Li et al., 2012; Boucher et al.*, 2013].

~~The purpose of this paper is to quantify the roles of convection and non-convective processes in governing the occurrence of cirrus clouds. We~~ Here, we focus on the tropics only, given that cirrus clouds are widespread in the tropics [e.g. *Sassen et al.*, 2008; *Heymsfield et al.*, 2017]. Furthermore, cirrus clouds in the tropical tropopause layer (TTL) ~~affects~~ affect the transport of air [*Corti et al.*, 2005, 2006; *Dinh and Fueglistaler*, 2014a] and water vapor [see e.g. *Wang et al.*, 1996; *Jensen et al.*, 2001; *Dinh and Fueglistaler*, 2014b] into the stratosphere, thereby affecting the concentration of water vapor in the stratosphere. Stratospheric water vapor ~~itself~~ plays a significant role in ~~the~~ Earth's radiative energy budget [*Forster and Shine, 2002; Solomon et al.*, 2010; *Dessler et al.*, 2013].

Cirrus clouds form by either freezing of liquid cloud droplets at temperatures above −38 °C or in situ nucleation of ice crystals from the vapor phase at temperatures below −38 °C [*Heymsfield et al.*, 2017]. Convection plays a complicated role in driving cirrus formation from both the liquid and vapor phases. Cirrus clouds that form by freezing of liquid droplets in mixed-phase clouds can be considered to originate from convection. On the other hand, not all cirrus clouds that form in situ from the vapor phase are driven by convection. In the tropics, the negative temperature anomalies that can drive ice nucleation arise from multiple convective and non-convective sources, including (i) the adiabatic or diabatic cooling at the top of deep convection [*Hartmann et al.*, 2001; *Sherwood et al.*, 2003; *Robinson and Sherwood*, 2006; *Kim et al.*, 2018; *Gasparini et al.*, 2019], (ii) the adiabatic cooling associated with the upwelling branch of the Brewer–Dobson circulation [BDC, *Holton et al.*, 1995], (iii) large-scale Kelvin and Rossby waves [*Boehm and Verlinde*, 2000; *Immler et al.*, 2008; *Fujiwara et al.*, 2009; *Virts et al.*, 2010] and small-scale gravity waves [*Garrett et al.*, 2004; *Dinh et al.*, 2016; *Kim et al.*, 2016; *Reinares Martínez et al.*, 2021], and (iv) midlatitude intrusions [*Waugh and Polvani*, 2000; *Taylor et al.*, 2011].

The percentage of tropical cirrus clouds that originate from convection has been estimated previously using a variety of methods, each with its own drawback and associated uncertainty. For example, *Wang and Dessler* [2012] classified cirrus in the TTL that have ice water contents (IWCs) exceed the ambient water vapor to be of convective origin. However, although cirrus of convective origin may have large IWCs at the beginning of their life cycles, subsequent processes such as ice sedimentation and sublimation, and cloud horizontal spreading ~~and ice sublimation~~ can decrease the IWC by several orders of magnitude [*Boehm et al., 1999; Luo and Rossow, 2004; Dinh et al.*, 2010, 2012~~, 2014~~; *Gehlot and Quaas, 2012; Dinh et al., 2014; Jensen et al., 2018; Gasparini et al., 2021*]. Another method is using low values of the outgoing longwave radiation (OLR) as a proxy for deep convection, and cirrus clouds located in regions of low OLRs can be considered to originate from convection [e.g., *Massie et al.*, 2002; *Dessler et al.*, 2006]. However, anvil cirrus may persist after the convection

has ceased, or they are blown off away from the convective cores. These clouds originate from convection but may not be classified as so using the local OLR proxy. A more sophisticated method to track cirrus clouds in relation to convection is using parcel trajectories. The trajectories are often initialized at the locations of the cirrus clouds and then calculated backward following the winds for a time period [*Pfister et al.*, 2001; *Massie et al.*, 2002; *Spang et al.*, 2002; *Mace et al.*, 2006]. If convection is encountered along the back trajectories, then the clouds at the initialized locations are assumed to be convectively generated. This assumption may overestimate the number of clouds that originate from convection. Even though the convection occurs before the clouds in the same trajectories, it may or may not be the cause for the occurrence of the clouds. ~~Furthermore, if a trajectory is needed to track every cloud, the calculation becomes computationally expensive for a large number of clouds over a large spatial and temporal domain. Other variations of the trajectory method were carried out by *Luo and Rossow* [2004] and *Ueyama et* al. [2015]. *Ueyama et* al. [2015] calculated backward trajectories that end at the tropopause while *Luo and Rossow* [2004] performed forward trajectories that start from deep convective events; both groups simulated the evolution of clouds along the trajectories~~ Finally, *Ueyama et al.* [2015, 2018] performed back trajectory calculations where each trajectory is coupled with a cloud microphysics model in the vertical. This setup allows them to model cloud microphysical processes as well as determine if the convection encountered in the trajectories leads to cirrus occurrence. The relationship between convection and clouds along the trajectories can be analyzed but the results are applicable to the simulated cloud population, rather than the observed cloud population.

Here, we propose a different method to ~~identify cirrus clouds of convective and non-convective origins. It hinges on the physical argument that convection results in a net upward transport of water vapor [*Sherwood et* al., 2010]~~classify cirrus clouds from which their relationship to convection can be inferred. Specifically, we distinguish the clouds that occur at times when the air contains more moisture than usual from those that occur in air that is colder and contains less moisture than usual. Let us label these two categories of clouds moist and dry cirrus, respectively. In the monthly data from the Cloud-Aerosol Lidar and Infrared Pathfinder Satellite Observation (CALIPSO) and the fifth generation reanalysis product of the European Centre for Medium-Range Weather Forecasts (ERA5), we find that the maximum occurrence of moist cirrus in the tropics is at around 14 km in altitude. This level coincides with the upper bound of the vertical extent of convection [*Takahashi and Luo*, 2012]~~Positive specific humidity (SPH) anomalies in the tropical upper troposphere, TTL and lower stratosphere can be in principle traced back to convection . Observational evidence supporting the role of convection in moistening~~ Furthermore, the seasonal cycle of moist cirrus is consistent with that of tropical precipitation. These results, together with existing observational evidence that convection has an overall moistening effect in the tropical upper troposphere, TTL, and lower stratosphere ~~is available [see~~ e.g. *Soden and Fu*, 1995; *Liao and Rind*, 1997; *Sassi et al.*, 2001; *Folkins and Martin*, 2005; *Wright et al.*, 2009; *Corti et al.*, 2008; *Schiller et al.*, 2009; *Jensen et* al., 2020]~~. Accordingly, we identify the cirrus clouds that occur at times when the air contains more moisture than usual to originate from convection. On the other hand, the cirrus clouds that occur when the local conditions are dry and cold are classified to be of non-convective origins. We find that the spatiotemporal distributions of cirrus clouds of convective and non-convective origins are distinct from each other~~, suggest that moist cirrus are driven by convection. In contrast, the spatiotemporal distribution of dry cirrus is distinct from that of tropical convection, suggesting that these clouds are unrelated to convection. The seasonal cycle of ~~the cirrus that originate~~

from convection dry cirrus in and above the TTL is consistent with that of tropical convection, while the cold point tropopause (CPT) temperature, and the seasonal cycle of the cirrus in the TTL that do not originate from convection dry cirrus below the TTL is consistent with that of the tropical cold point tropopause (CPT). These results suggest that the new method is indeed appropriate for the purpose of identifying clouds of convective and non-convective origins. wave activities in the troposphere.

The knowledge that tropical cirrus clouds are driven by convection as well as by negative temperature anomalies associated with non-convective processes is not new (see the references cited above). However, to the best of our knowledge, this is the first time that individual vertical profiles of moist cirrus (that are related to convection) and dry cirrus (that are unrelated to convection) are obtained from observational data. In previous observational studies, a particular altitude (typically around 14 km–15 km, the bottom of the TTL) was chosen as a threshold level to separate cirrus driven by convection at lower altitudes and those which are driven by negative temperature anomalies at higher altitudes. Such a clear-cut separation may not be appropriate as the vertical profiles of moist and dry cirrus that we obtain here suggest that convection and non-convective sources contribute almost equally to the total occurrence of cirrus clouds above 14 km. Furthermore, the vertical profile of dry cirrus reveals that a significant number of cirrus clouds in the troposphere are formed by negative temperature anomalies unrelated to convection. Much of previous research on the effect of temperature anomalies on cirrus clouds has focused on the higher altitudes in and above the TTL only. The other significant finding is that moist and dry cirrus contain similar IWCs if they are located at the same altitude or temperature level. Previously, cirrus that originate from convection were often thought to have larger IWCs [see e.g. *Wang and Dessler*, 2012].

The remaining of the paper is organized as follows. The data and methodology are described respectively in Sections 2 and 3. Section 4 discusses the characteristics of the occurrence of tropical cirrus of convective and non-convective originsmoist and dry cirrus in the tropics, including their spatiotemporal distributions and IWCs. Section 5 contains the summary.

2 Data

We analyze the monthly-mean, three-dimensional cirrus cloud occurrence and IWC of the Lidar Level 3 Ice Cloud Data, Standard Version 1-00 [*NASA Langley Atmospheric Science Data Center*, 2018]. This data was collected with the Cloud-Aerosol LIdar with Orthogonal Polarization (CALIOP) instrument on the Cloud-Aerosol Lidar and Infrared Pathfinder Satellite Observation CALIPSO , CALIPSO [*Winker et al.*, 2010]. CALIOP is capable of detecting clouds with optical depths of 0.01 or less [*Winker et al.*, 2007]. For this reason, CALIOP data are well suited for studies of cirrus clouds, many of which are optically thin. The user guides for the monthly Lidar Level 3 Ice Cloud Data can be found online (see https://www-calipso.larc.nasa.gov/resources/calipso_users_guide/qs/cal_lid_l3_ice_cloud_v1-00.php and https://www-calipso.larc.nasa.gov/resources/calipso_users_guide/qs/cal_lid_l3_cloud_occurrence_v1-00.php).

The spatial resolution of the monthly Lidar Level 3 Ice Cloud Data is 2.5° in the zonal direction, 2.0° in the meridional direction, and 120 m in the vertical. The monthly data is not suitable to conduct case study of clouds that occur in response to individual convection or wave events. However, if convection and wave activities have intrinsic seasonal cycles, their effects on the seasonal cycles of cirrus occurrence should be captured in the monthly data. Thus, this data is appropriate for us to study the

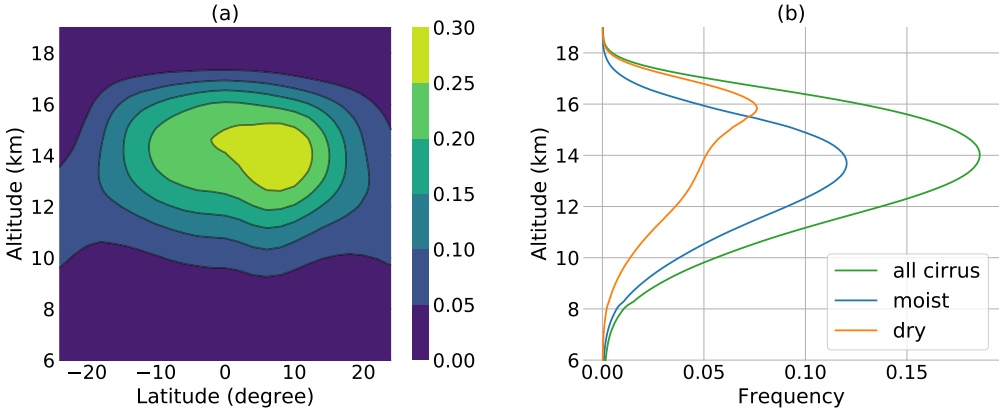

Figure 1. Climatological mean frequency of occurrence of cirrus clouds in the tropics: (a) latitude–altitude profile of the zonal mean frequency of occurrence, and (b) vertical profile of the frequency of occurrence averaged over the tropics.

spatial distribution of cirrus clouds on the seasonal and climatological time scales. Figure 1 shows the frequency of occurrence of cirrus clouds in the tropics between 24 °S and 24 °N over the 9-year period from January 2007 to December 2015 obtained from CALIPSO. The overall spatial distribution of cirrus clouds in the figure is consistent with previous observational studies using CALIPSO [*Sassen et al.*, 2008; *Mace et al.*, 2009; *Hong and Liu*, 2015] and satellite radiometers [*Wang et al.*, 1996].

~~To study~~ For the meteorological conditions surrounding cirrus clouds, ~~we analyze the temperature and SPH~~specifically the specific humidity (SPH) and temperature of the atmosphere~~. For these~~, we use the ~~fifth generation reanalysis product (~~ERA5 ~~) of the European Centre for Medium-Range Weather Forecasts (ECMWF)~~data [*Hersbach et* al., 2020]. In addition, we obtain the data for precipitation from the Version-2 Global Precipitation Climatology Project (GPCP) Monthly Precipitation Analysis [*Adler et al.*, 2003]. The ~~temperature, SPH,~~ SPH, temperature, and precipitation data were downloaded for the same temporal and spatial domains as the ice cloud data above, and then they were interpolated to the same grid as the ice cloud data.

3 Identifying ~~cirrus of convective~~ moist and ~~non-convective origins~~dry cirrus

Figure 2 shows the vertical profiles of the relative humidity (RH) that has been averaged over time and the tropical domain in cloudy and ~~cloud-free~~ all-sky conditions. The RH discussed in this work is specifically with respect to ice. At a given grid box location, ~~the~~ cloudy conditions refer to the times when cirrus clouds are detected~~in the grid box. The cloud-free conditions refer to the remaining times when the grid box is cloud-free~~, i.e., when the ice cloud fraction is greater than 0.01, in the grid box. The figure shows that on average the RH is greater in cloudy conditions than in ~~cloud-free~~ all-sky conditions at every altitude. This is consistent with existing observations [*Sandor et al.*, 2000; *Kahn et al.*, 2008, 2009; *Krämer et al.*, 2020] that the RH is greater in cloudy conditions to support the formation and maintenance of ~~the~~ clouds.

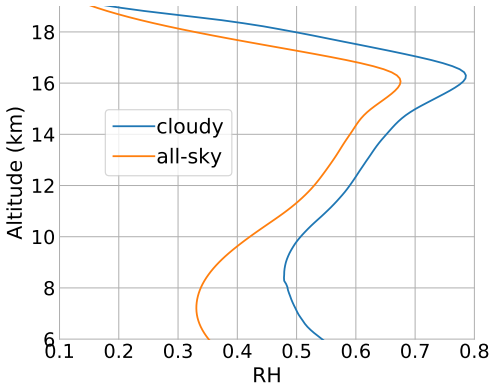

Figure 2. Vertical profiles of the climatological tropical mean RH in cloudy and ~~cloud-free~~ all-sky conditions~~averaged over the tropics~~.

The RH is related to the temperature (T) and the SPH (q) via

$$\mathrm{RH} = \frac{p_\mathrm{v}}{e_\mathrm{si}(T)} = \frac{R_\mathrm{v}}{R}\frac{q}{e_\mathrm{si}(T)}p, \tag{1}$$

where $R = 287\,\mathrm{J\,kg^{-1}\,K^{-1}}$ and $R_\mathrm{v} = 461\,\mathrm{J\,kg^{-1}\,K^{-1}}$ are respectively the specific gas constants of air and water vapor, p is atmospheric pressure, p_v is the partial pressure of water vapor in air, and $e_\mathrm{si}(T)$ is the saturation water vapor pressure with respect to ice, a function of temperature. The function $e_\mathrm{si}(T)$ increases with temperature and is calculated based on the empirical formula given by *Murphy and Koop* [2005]. According to Eq. (1), at a given pressure level, large RH values inside clouds relative to ~~cloud-free conditions~~ the all-sky condition must arise from positive SPH anomalies and/or negative temperature anomalies.

~~Let $\Delta q(x,y,z,t) = q_\mathrm{cld}(x,y,z,t) - \overline{q_\mathrm{cfr}}(x,y,z)$~~ Let $\Delta q(x,y,z,t) = q_\mathrm{cld}(x,y,z,t) - \overline{q}(x,y,z)$ denote the difference between the SPH in the cloud sample at the location (x,y,z) and time t and the ~~average SPH in cloud-free conditions~~ time-average SPH at the same location. The ~~average cloud-free SPH ($\overline{q_\mathrm{cfr}}$~~time-average SPH ($\overline{q}$) is obtained by averaging the SPH over ~~the times when that location is cloud-free~~all the times in the dataset regardless of whether clouds are present in the grid box. Similarly, ~~$\Delta T(x,y,z,t) = T_\mathrm{cld}(x,y,z,t) - \overline{T_\mathrm{cfr}}(x,y,z)$~~ $\Delta T(x,y,z,t) = T_\mathrm{cld}(x,y,z,t) - \overline{T}(x,y,z)$ is the difference between the temperature in the cloud sample at the location (x,y,z) and time t and the ~~average temperature in cloud-free conditions~~ time-average temperature at the same location. The vertical profiles of the climatological mean, tropical average Δq and ΔT are shown in Fig. 3. The figure shows that Δq (green line) is positive in the troposphere, indicating that most cirrus clouds in the troposphere are formed and maintained in the months of positive SPH anomalies. Furthermore, Δq decreases exponentially with altitude, consistent with the fact that the background SPH decreases exponentially with altitude. On the other hand, the magnitude of the temperature anomalies experienced by cirrus clouds is small in most of the troposphere, and it becomes significant only above 14 km or so. The result that cirrus clouds above 14 km experience significant negative temperature anomalies is consistent with previous studies [*Boehm and Verlinde*, 2000; *Virts et al.*, 2010; *Virts and Wallace*, 2010; *Tseng and Fu*, 2017].

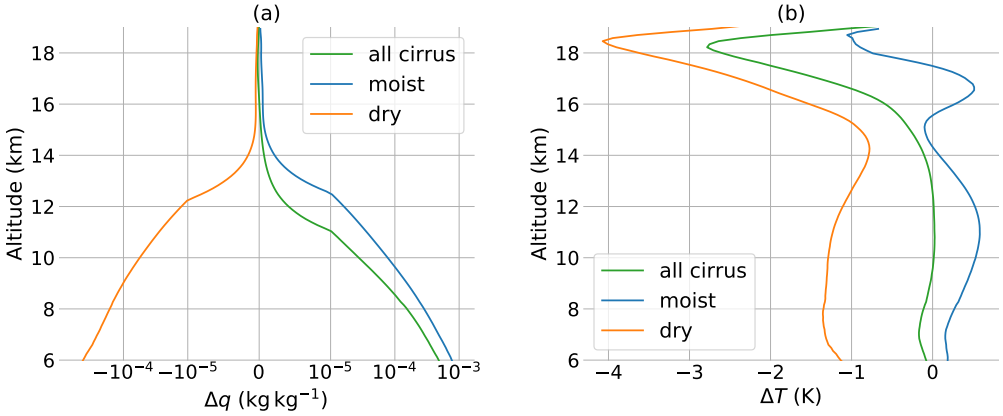

Figure 3. Vertical profiles of the climatological mean, tropical average differences in (a) SPH and (b) temperature between cloudy and ~~cloud-free~~ all-sky conditions.

~~Histogram of cloud samples against the differences in SPH and temperature between cloudy and cloud-free conditions.~~

~~In the free troposphere,~~ Let us refer to the clouds in which $\Delta q > 0$ as moist cirrus. We expect that moist cirrus are influenced by convection since positive SPH anomalies are largely produced by the upward transport of moisture by convection in the free atmosphere in the tropics. Some positive SPH anomalies may be located away from active convection, but even in these cases the source of moisture must be the convective outflows that have been transported horizontally by the winds [see *Salathé and Hartmann*, 1997; *Sohn et al.*, 2008; *Das et al.*, 2011]. ~~Therefore, we identify the clouds in which $\Delta q > 0$ to be of convective origin, hereafter 'convective' cirrus. Our definition of convective cirrus includes~~ Moist cirrus include clouds that form within the convective updrafts and at the top of convection, as well as those that form in the moist air of the convective outflows downstream of convection. Examples of the latter type of ~~convective~~ moist cirrus were recently reported by *Cairo et al.* [2021]. Using this ~~method~~definition, we find that ~~66 %~~ 58 % of tropical cirrus clouds are ~~convective~~ moist cirrus (see Fig. 4). About ~~half of the convective~~ 60 % of moist cirrus experience positive temperature anomalies, and the ~~other half~~ remaining 40 % experience negative temperature anomalies.

The remaining cirrus clouds in which $\Delta q \leq 0$ consist of two categories. The first category comprises of the cloud samples in which $\Delta q \leq 0$ and $\Delta T < 0$. ~~This makes up 24 %~~ We refer to these clouds as dry cirrus. Dry cirrus make up 34 % of tropical cirrus clouds (see Fig. 4). ~~As these clouds coincide with dry anomalies~~Since convection sometimes leads to dehydration of the air [*Jensen et* al., 2007], in principle some dry cirrus can be associated with convection. However, our analysis (see Section 4.2) shows that the monthly spatiotemporal distribution of dry cirrus is distinct from those of convection and moist cirrus. The maximum frequency of occurrence of dry cirrus is located remotely away from the maximum frequency of occurrence of moist cirrus. Thus, the negative temperature anomalies that form and maintain ~~these clouds~~ dry cirrus are unlikely to be the cooling at the top of convection. Rather, they are associated with waves and/or the adiabatic cooling associated with the upwelling of the BDC. ~~Even though some waves are generated by convection, the impact of convection on these clouds through wave generation~~

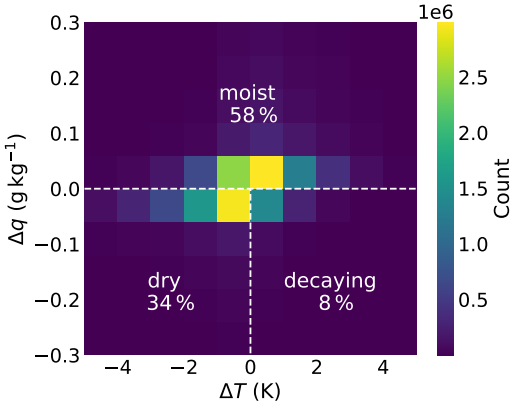

Figure 4. Histogram of cloud samples against the differences in SPH and temperature between cloudy and all-sky conditions.

~~is indirect only. We therefore label these clouds 'non-convective' cirrus.~~ The last category of clouds is for those in which $\Delta q \leq 0$ and $\Delta T \geq 0$. These clouds are ~~neither driven by~~ driven by neither positive SPH anomalies nor negative temperature anomalies. They are most likely in the decaying stage of their lifetimes. In these cases, the SPH and temperature anomalies cannot be used to identify their formation and maintenance mechanisms. ~~These clouds are labeled 'unidentified'.~~

~~With the unidentified clouds comprising only 10 %~~ Decaying clouds make up 8 % of tropical cirrus ~~clouds, the method described above allows us to identify the majority of cirrus clouds and their relationship with convection.Furthermore, as shown in Section 4 below, the spatial distributions and seasonal cycles of convective and non-convective cirrus are distinct from each other. The occurrence of convective cirrus is consistent with the location and the seasonal cycle of tropical convection, while the occurrence of non-convective cirrus is consistent with the CPT. The seasonal cycle of the CPT is strongly coupled to that of the BDC *Highwood and Hoskins*, 1998; *Jucker and Gerber*, 2017. These results suggest that the method we propose is appropriate to separate convective and non-convective cirrus~~(see Fig. 4).

4 Characteristics of the occurrence of ~~convective~~ moist and ~~non-convective~~ dry cirrus

4.1 Spatial distributions

Figures 1 and 5 ~~(a)~~ show that the frequency of occurrence of ~~convective~~ moist cirrus is maximum ~~at around~~ near 14 km (∼ 150 hPa), coincided with the level of zero net radiative heating rate, which is often defined as the bottom of the TTL [*Fueglistaler et al.*, 2009]. The 14 km altitude is also approximately the level of neutral buoyancy, which provides the upper bound for convective development in the vertical [*Takahashi and Luo*, 2012]. The level of maximum convective mass outflow is located several kilometers lower at around 10 km–11 km [*Takahashi and Luo*, 2012]. ~~Convective~~ Moist cirrus between the level of neutral buoyancy (14 km) and the level of maximum convective outflow (10 km–11 km) are likely anvil cirrus. ~~Convective~~ Moist cirrus above 14 km are likely to originate from (i) the further lofting, spreading and detachment of anvils, (ii) in situ ice

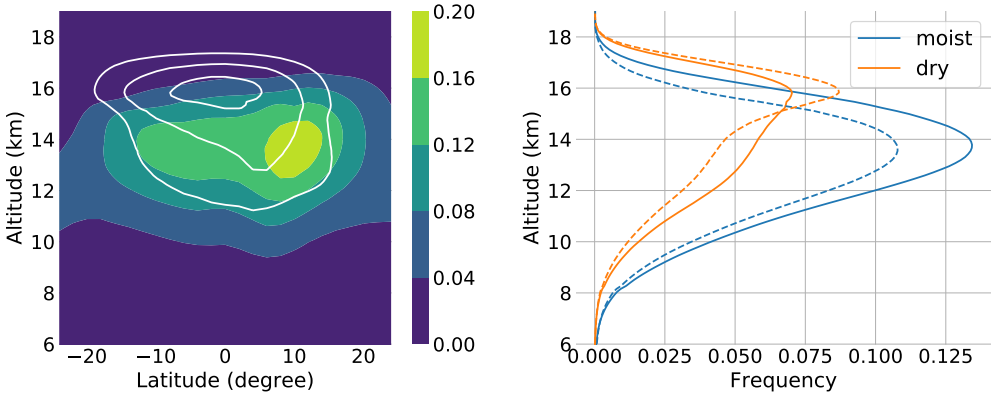

Figure 5. (a) Latitude–altitude profiles of the climatological zonal mean frequency of occurrence of moist cirrus (~~top~~filled colored contours) and ~~grid-average ice mass density in the domain~~ dry cirrus (~~g m^{-3}~~white contours), ~~bottom~~and (b) vertical profiles of ~~convective~~ the climatological zonal mean frequency of occurrence of moist and dry cirrus averaged over the SH (~~left~~dashed) and ~~non-convective cirrus~~ NH (~~right~~solid).

nucleation in the moist air of the convective outflows in response to cold anomalies (see Fig. 3) associated with the cooling at the top of deep convection and/or waves. At lower altitudes (below 10 km or at temperatures above 235 K), ~~convective~~ moist cirrus originate from mixed-phase clouds [*Heymsfield et al.*, 2017], i.e. they are of liquid origin [terminology following *Krämer et al.*, 2016]. ~~Convective cirrus below 14 km tend to~~ More moist cirrus experience positive temperature anomalies ~~(see Fig~~than negative temperature anomalies (see Figs. 3~~), most likely associated with~~ b and 4). The positive temperature anomalies likely arise from the latent heat release in convection.

~~Non-convective~~ Dry cirrus tend to occur at higher altitudes than ~~convective~~ moist cirrus. The frequency of occurrence of ~~non-convective~~ dry cirrus maximizes at around 16 km, below the CPT (see Figs. 1 and 5~~b~~). The climatological tropical mean CPT is found to be at 16.8 km. The level of maximum cirrus occurrence is capped above by the CPT potentially because of two reasons. Firstly, the RH decreases with altitude above the CPT as temperature increases with altitude (see Fig. 2). Thus, above the CPT the negative temperature perturbations must be of large magnitudes to raise the RH above the threshold of ice nucleation. Secondly, the modelling study by *Dinh et* al. [2010] suggested that a necessary condition for cirrus clouds to self-maintain for a long time is that the temperature in the cloud layer decreases with altitude. In this situation, the circulation induced by the cloud radiative heating produces in-cloud water vapor flux convergence that acts against ice sublimation [*Dinh et al.*, 2010]. On the other hand, when the temperature in the cloud layer increases with altitude (such as above the CPT), the circulation induced by the cloud radiative heating produces in-cloud water vapor flux divergence that enhances ice sublimation. ~~This means that~~ As a result, clouds above the CPT are short-lived and ~~as a result,~~ so the frequency of cloud occurrence above the CPT is small.

Table 1. Percentage contributions of the different types of cirrus clouds to the total cirrus occurrence in different layers of the tropical atmosphere. The bottom of the tropical tropopause layer (TTL) is located near 14.0 km (∼ 150 hPa). The climatological tropical mean CPT is at 16.8 km (∼ 100 hPa).

	~~Convective~~ Moist	~~Non-convective~~ Dry	~~Unidentified~~Decaying
Above CPT	~~23~~ 22	76	~~1~~2
Above 16.8 km	25	73	2
Above 14.0 km	~~49~~ 48	~~44~~ 46	6
Below 14.0 km	67	26	7
All altitudes	~~66~~ 58	~~24~~ 34	~~10~~ 8

Table 1 shows the percentage contributions of the different types of cirrus clouds to the total cirrus in different layers of the tropical atmosphere. The table shows that ~~convective~~ moist cirrus dominate the entire atmosphere and the troposphere below 14 km, i.e., the bottom of the TTL. Above 14 km, ~~convective and non-convective~~ moist and dry cirrus contribute almost equally to the total cirrus cloud occurrence~~, a result consistent with~~ . This is consistent with the observational study by *Massie et al.* [2002] that convection affects half of cirrus population in the TTL, although they studied cirrus clouds over the maritime continent only. This result is also consistent with the modeling study by *Schoeberl et* al. [2018] in which cirrus cloud fraction in the TTL doubles when convection is included in the model simulations. Above the CPT, ~~non-convective~~ dry cirrus make up the large majority (76 %) of clouds, but the percentage of ~~convective~~ moist cirrus is not negligible (~~23 %). Note that these results were obtained for the spatially and temporally varying CPT, rather than~~ 22 %). Similar numbers (73 % dry cirrus and 25 % moist cirrus) are obtained above 16.8 km, which is the altitude of the climatological tropical mean CPT~~at 16.8 km.~~ .

~~Based on the vertical profile of the frequency of occurrence of convective cirrus clouds (see Fig. 1b) , we can estimate the degree of overshooting convection above the CPT. Above the CPT, the frequency of occurrence of convective cirrus decreases with altitude, indicating that the degree of penetration of convection into the stratosphere decreases with altitude. At the CPT, the frequency of occurrence of convective cirrus is 1.7 %. This provides the upper bound for the occurrence of overshooting convection injecting ice into the stratosphere because not all convective cirrus are formed within the convective updrafts; some convective cirrus are formed in situ in the moist air of the convective ouflows. *Gettelman et* al. [2002] found based on cloud brightness temperatures that convection is present above the CPT about 0.5 % of~~

Figure 5 shows that there are more moist cirrus clouds in the Northern Hemisphere (NH) than in the Southern Hemisphere (SH) at every altitude. This is consistent with the ~~time~~fact that convection is tronger in the NH than in the SH. On the other hand, above 15 km there are less dry cirrus clouds in the NH than in the SH, and below 15 km there are more dry cirrus clouds in the NH than in the SH. Above 15 km, the occurrence of dry cirrus is anti-correlated with the CPT temperature, which is ~~indeed less than the upper bound estimated here.~~

~~Frequency of occurrence of convective and non-convective cirrus clouds: (a) latitudinal profile of the vertical maximum of the climatological zonal mean frequency and (b) climatological monthly profile of the vertical maximum frequency averaged over the tropics.~~

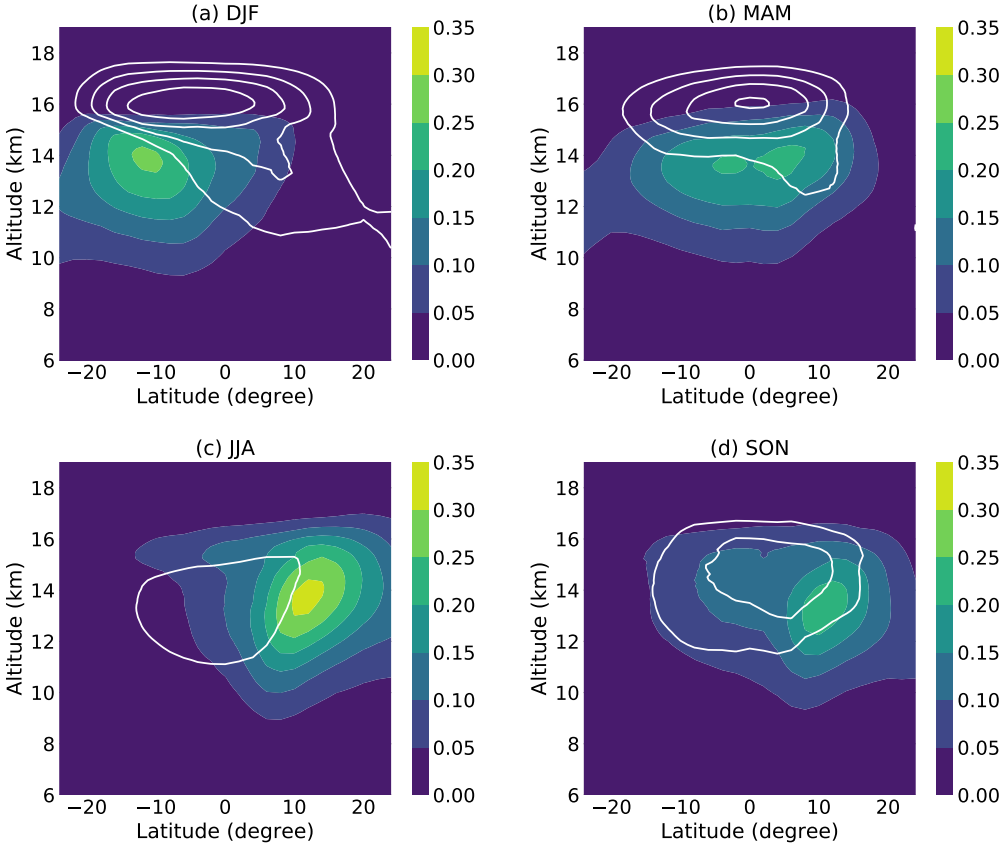

Figure 6. Latitude–altitude profiles of the zonal mean frequency of occurrence of moist cirrus (filled colored contours) and dry cirrus (white contours) in December–January–February (DJF), March–April–May (MAM), June–July–August (JJA), and September–October–November (SON).

~~The meridional pattern of convective cirrus occurrence is bimodal and asymmetric about the equator (Figs. 5a and ??). There are two maxima at approximately 10 °S and 10 °N, with the northern hemisphere (NH) maximum being larger than the southern hemisphere (SH) maximum, consistent with the fact that convection is stronger in the NH. In comparison, the meridional pattern of non-convective cirrus occurrence is unimodal, with the maximum frequency of occurrence centered around the equator (Figs. 5b and ??). The different spatial distributions of convective and non-convective cirrus suggest that the mechanisms governing the occurrence of non-convective cirrus is distinct from convection . This topic is further discussed in Section 4.2.~~

~~Figures 5(c) and (d) show the grid-average ice mass density associated with convective and non-convective cirrus. For both types of clouds~~controlled by the upwelling of the BDC. The maximum center of the upwelling of the BDC is located in the SH [*Mote et* al., 1996; *Plumb and Eluszkiewicz*, 1999], so there are more dry cirrus in the SH above 15 km. To explain why below 15 km there are more dry cirrus clouds in the NH than the SH, ~~the maximum ice mass density is located below~~ we refer to Fig. 6

which shows the occurrence of moist and dry cirrus over the four seasons. In the ~~maximum frequency of occurrence. This is because cirrus clouds at lower altitudes (higher temperatures) contain more IWCs (more on this in Section 4.3). Interestingly, Fig. 5(d) reveals that non-convective cirrus in the troposphere contribute significantly to the ice mass in the domain. These~~ NH, dry cirrus below 15 km occur most frequently in the boreal winter (December–January–February) and to a lesser extent in the boreal spring (March–April–May). In these months of the year, convection is the least active in the NH and the most active in the SH, consistently with the distribution of moist cirrus clouds shown in Fig. 6. In other words, dry cirrus below 15 km are located remotely away (in the opposite hemisphere) from the most active convection. It is thus unlikely that dry cirrus clouds below 15 km are driven by convection, even though convection can produce negative temperature anomalies. We posit that these low-altitude ~~non-convective cirrus occur much less frequently than their non-convective counterpart in the TTL (see Fig. 1b)~~dry cirrus are instead driven by the temperature anomalies associated with gravity waves in the troposphere. Observations of gravity waves in the tropical troposphere are rare. However, ~~they contain significantly higher IWCs than high-altitude cirrus clouds. Low-altitude non-convective cirrus are located at higher latitudes towards the northern and southern edges of the tropics, in contrast to high-altitude non-convective cirrus which are located near the equator (comparing Figs. 5b and d)~~the particular radiosonde data over the tropical regions of the USA [*Zhang et* al., 2010] indeed show that the energy density of tropospheric gravity waves is maximum in the boreal winter–spring, consistent with the occurrence of low-altitude dry cirrus in the NH in these seasons.

4.2 Seasonal cycles

Figure 7 shows how the seasonal cycle of ~~convective~~ moist cirrus is forced from the bottom up by the seasonal cycle of the SPH in the troposphere, while the seasonal cycle of ~~non-convective cirrus~~ dry cirrus in the TTL is forced from the top down by the seasonal cycle of the temperature in the TTL and lower stratosphere. In each hemisphere, ~~convective~~ moist cirrus occur most ~~(least)~~ frequently during the summer ~~(winter)~~ months when the SPH perturbations are positive ~~(negative)~~and least frequently during the winter months when the SPH perturbations are negative. The seasonal cycle of ~~convective~~ moist cirrus in the NH is thus opposite of that in the SH, i.e., when the frequency of occurrence of ~~convective~~ moist cirrus is maximum in the NH, it is minimum in the SH. ~~The net result is that over the entire tropics, the frequency of occurrence of convective cirrus is roughly constant (Fig. **??**b).~~ In contrast, in both the NH and SH ~~non-convective~~ dry cirrus occur most ~~(least)~~ frequently in the boreal winter ~~(summer)~~ when the temperatures in the TTL are minimum ~~(maximum). The net result is that over the entire tropics, the frequency of occurrence of non-convective cirrus has a strong seasonal cycle with a maximum in the boreal winter and a minimum~~ and least frequently in the boreal summer ~~(Fig. **??**b)~~when the temperatures in the TTL are maximum.

~~Climatological monthly zonal mean frequency of occurrence of convective cirrus (left) and non-convective cirrus (right) over the SH (top) and NH (bottom). Shown with black contours are the monthly SPH perturbations relative to the annual mean SPH (left), and the monthly temperature perturbations relative to the annual mean temperature (right). Positive (negative) SPH and temperature perturbations are shown with solid (dashed) contours.~~

Figure 8(a) shows the seasonal migrations of ~~convective~~ moist cirrus and precipitation between the NH in the boreal winter and the SH in the austral summer. The similar seasonal patterns of ~~convective~~ moist cirrus and precipitation suggest that these

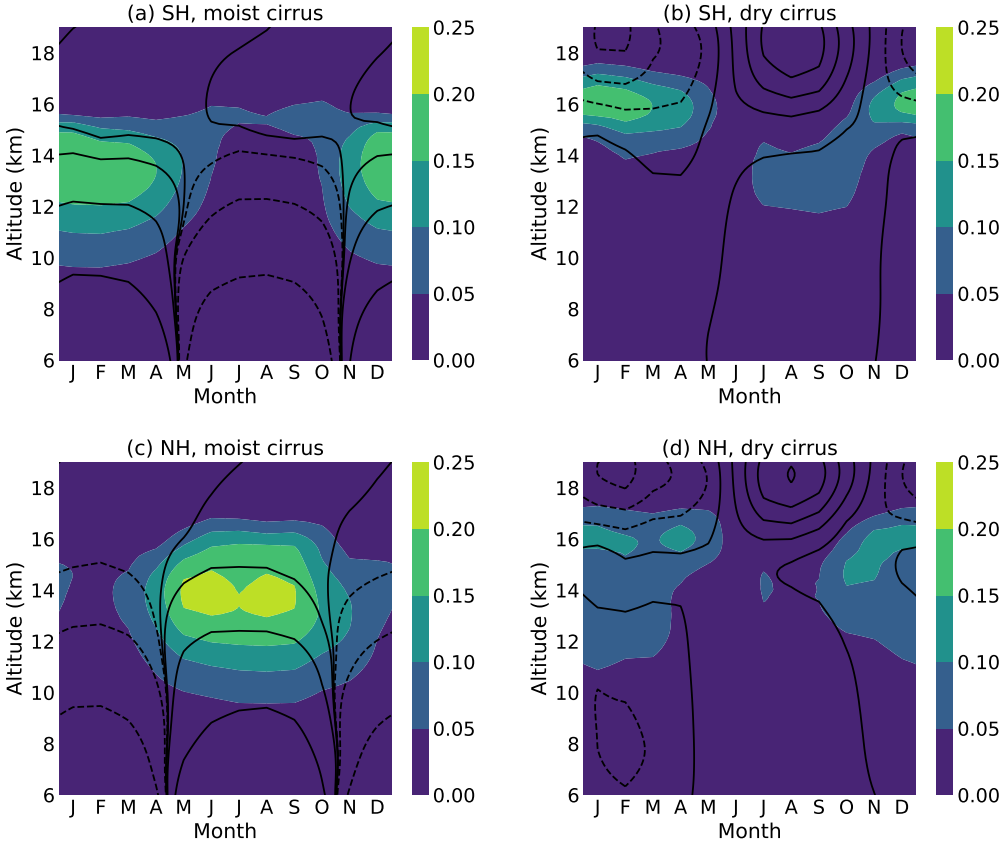

Figure 7. Monthly zonal mean frequency of occurrence of moist cirrus (left) and dry cirrus (right) over the SH (top) and NH (bottom). Shown with black contours are the monthly SPH variations relative to the annual mean SPH (left), and the monthly temperature variations relative to the annual mean temperature (right). Nonnegative SPH and temperature variations are shown with solid contours, and negative SPH and temperature variations are shown with solid contours.

clouds are indeed coupled to tropical convection. The seasonal variations of ~~convective~~ moist cirrus are thus controlled by the seasonally varying Hadley cells, the intertropical convergence zones (ITCZ), and monsoons. The maximum frequency of occurrence of ~~convective~~ moist cirrus clouds occur at around ~~10 °N~~ 11 °N–12 °N in the boreal summer and ~~10 °N~~ 11 °S–12 °S in the austral summer, with the boreal summer maximum larger than the austral summer maximum. The asymmetry between the NH and SH maxima is associated with the asymmetry of the ITCZ, which arises from the different shapes of the continents in the NH and SH [*Xie*, 2004]. ~~Overall, there are more convective cirrus in the NH (~60 %) than the SH (~40 %).~~

~~In contrast to convective cirrus , non-convective cirrus occur most frequently~~ While the pattern of moist cirrus occurrence migrates between the NH and SH seasonally, the pattern of dry cirrus occurrence does not move significantly in the meridional direction with seasons. Dry cirrus obtain a single but broad maximum frequency of occurrence in the boreal ~~winter near~~ winter–spring within 10° of the equator (see ~~Fig.~~ Figs. 6 and 8b). ~~The~~ Figure 8(b) further shows that the seasonal pattern of

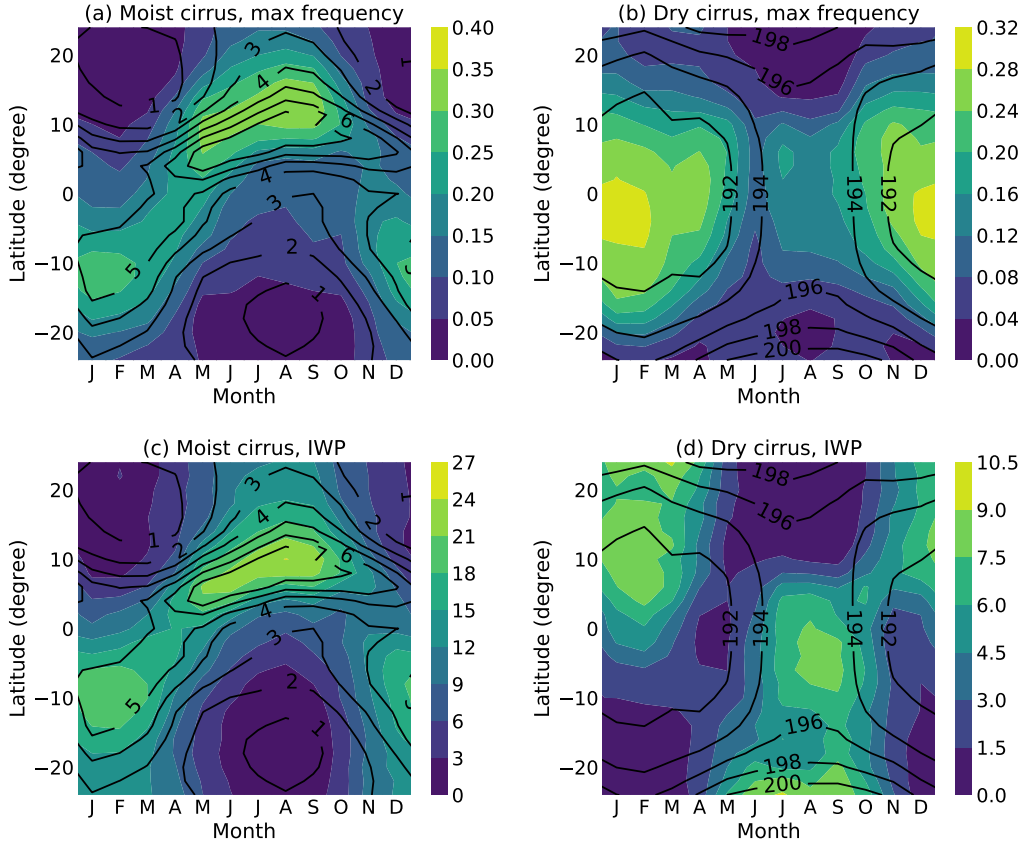

Figure 8. Monthly–meridional distributions of the vertical maximum, zonal mean frequency of cirrus occurrence (top), and the zonal mean ice water path (IWP in $g\,m^{-2}$, bottom). The left panels show ~~convective~~ moist cirrus with the zonal mean precipitation ($mm\,d^{-1}$) in black contours, and the right panels show ~~non-convective~~ dry cirrus with the zonal mean CPT temperature (K) in black contours.

~~non-convective~~ the vertical maximum of dry cirrus occurrence is negatively correlated with the seasonal pattern of the CPT temperature. The vertical maximum of the frequency of occurrence of dry cirrus is located at around 16 km (recall Fig. 1b), so Fig. 8(b) generally captures the behavior of dry cirrus at high altitudes in the TTL and lower stratosphere. The seasonal cycle of the CPT is driven by the seasonal cycle of stratospheric planetary waves in the extratropical latitudes [*Yulaeva et al.*, 1994; *Highwood and Hoskins*, 1998; *Jucker and Gerber*, 2017]. During the boreal winter, stronger wave activities in the extratropics result in stronger upwelling of the BDC and lower CPT temperatures [*Yulaeva et al.*, 1994; *Holton et al.*, 1995; *Highwood and Hoskins*, 1998]. In the cold TTL during the boreal winter, local negative temperature perturbations such as those generated by waves can readily increase the RH above the threshold for ice nucleation and so clouds are formed frequently. ~~Figure 8(b) further shows that there are more non-convective cirrus in the SH than the NH. The reason for this is that the~~ The maximum center of the upwelling of the BDC is located in the SH in the boreal winter [*Mote et al.*, 1996; *Plumb and Eluszkiewicz*, 1999], so the maximum frequency of occurrence of dry cirrus also occurs in the SH in the boreal winter.

The seasonal cycles of ~~convective and non-convective cirrus described here~~ moist and high-altitude dry cirrus described above are generally consistent with previous studies of cirrus clouds below 14 km–15 km [*Sassen et al.*, 2008; *Virts and Wallace*, 2010; *Nee and Lu*, 2021] and cirrus clouds above 14 km–15 km [*Tseng and Fu*, 2017; *Nee and Lu*, 2021], respectively. However, the significance here is that we are able to distinguish ~~convective and non-convective~~ moist and dry cirrus from each other despite the overlapping in their vertical distributions (see Fig. 1b). By separating ~~convective and non-convective~~ moist and dry cirrus from each other, we can clearly demonstrate the relationships between ~~convective~~ moist cirrus and convection, and between ~~non-convective cirrus~~ high-altitude dry cirrus and the temperature in the TTL and ~~the temperature there~~lower stratosphere. In previous studies, a particular altitude level (typically around 14 km–15 km) was chosen as a threshold to separate low- and high-altitude cirrus. In addition, much of previous research on the effect of temperature anomalies on cirrus clouds has focused on the higher altitudes in and above the TTL only. Here, the vertical profile of dry cirrus (see Fig. 1b) reveals a population of dry cirrus driven by negative temperature anomalies in the troposphere. We will return to discuss these low-altitude dry cirrus clouds in the troposphere in Section 4.3 below.

4.3 Ice water contents

Figure 9 shows the distributions of the occurrence of ~~convective and non-convective~~ moist and dry cirrus against temperature and in-cloud IWC. The frequency of occurrence of ~~convective~~ moist cirrus is maximum in the temperature range between ~~200 K~~ 210 K and 250 K, with IWCs between ~~10^{-3} g m^{-3}~~ 10^{-2} g m^{-3} and 10^{-1} g m^{-3}. In comparison, the histogram of ~~non-convective~~ dry cirrus shows a distinct maximum count between 190 K and 200 K, which is around the CPT temperature. The IWC of the peak distribution of ~~non-convective~~ dry cirrus is between ~~10^{-5} g m^{-3}~~ 10^{-4} g m^{-3} and 10^{-3} g m^{-3}. However, ~~non-convective~~ dry cirrus are also occasionally detected below the TTL at temperatures above 200 K (altitudes below 14 km, see also Fig. 1b). These ~~non-convective~~ dry cirrus at low altitudes have IWCs comparable to those of ~~convective~~ moist cirrus at the same temperature/altitude levels.

Figure 9 further shows that the IWC in cirrus clouds increases with increasing temperature (decreasing altitude), which is consistent with previous observations [*Schiller et al.*, 2008; *Krämer et al.*, 2016; *Heymsfield et al.*, 2017; *Krämer et al.*, 2020]. The behavior of the in-cloud IWC as an increasing function of temperature holds regardless whether the clouds are ~~convective or non-convective~~ moist or dry cirrus. Thus, ~~non-convective~~ dry cirrus typically contain less ice water than ~~convective cirrus because non-convective~~ moist cirrus because dry cirrus typically form at lower temperatures (higher altitudes). The different formation mechanisms (convection or non-convective processes) govern the temperature range in which cirrus clouds are formed, through which they govern the IWC ~~of~~ in the clouds.

As a consequence of the in-cloud IWC being a function of temperature regardless of cloud types, the vertical profiles of the in-cloud IWC of moist and dry cirrus are very similar (see the dashed lines in Fig. 10).

~~Figure 10 shows that the domain-average ice mass density of non-convective~~ On the other hand, the grid-average IWC due to dry cirrus is about an order of magnitude less than that ~~of convective~~ due to moist cirrus throughout most of the atmosphere except above about 15.5 km ~~. The domain-average ice mass density~~ (see the solid lines in Fig. 10). The grid-average IWC depends on both the in-cloud IWC and the frequency of occurrence of clouds. Given that the IWCs in ~~convective and~~

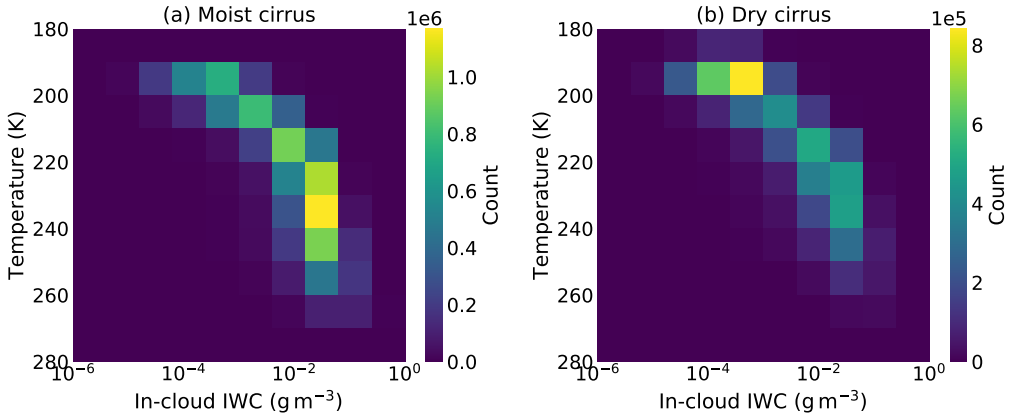

Figure 9. Histogram of cloud samples against temperature and in-cloud IWC for (a) ~~convective~~ moist cirrus and (b) ~~non-convective~~ dry cirrus.

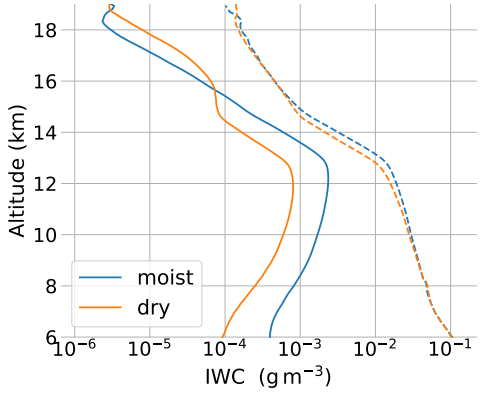

Figure 10. Vertical profiles of the ~~ice mass density averaged over the~~ climatological tropical ~~domain due to convective~~ mean grid-average IWC (solid) and ~~non-convective~~ in-cloud IWC (dashed) associated with moist and dry cirrus.

non-convective moist and dry cirrus are comparable (at least in the same order of magnitude) to each other at each temperature/altitude level(Fig. 9), the difference in the domain-average ice mass density between convective and non-convective grid-average IWC between moist and dry cirrus is determined mainly by the difference in the frequency of occurrence between the two types of clouds. The 15.5 km level marks the altitude above which the frequency of occurrence (see Fig. 1b) and therefore the domain-average ice mass density of non-convective grid-average IWC of dry cirrus exceed those of convective moist cirrus.

Finally, Figs. 8(c) and (d) show the seasonal cycle of the ice water path (IWP) in the domain due to convective and non-convective due to moist and dry cirrus. The IWP is dominated by the ice water at low altitudes (see Fig. 10). Therefore, the seasonal cycle of the IWP reflects the seasonal cycle of cirrus clouds at low altitudes. For convective moist cirrus, the seasonal patterns of the IWP and the maximum frequency of occurrence located at 14 km (see Fig. 1b) are similar. This indicates that convective moist cirrus throughout the troposphere are coupled to each other and to convection. On the other hand, for non-convective by comparing Figs. 8(b) and (d), we can see that, for dry cirrus, the seasonal pattern of the IWP is different from that of the occurrence frequency maximum vertical maximum of the frequency of occurrence (which is located at near 16 km in the TTL, see Fig. 1b). Low-altitude non-convective While high-altitude dry cirrus are mostly located in the deep tropics, low-altitude dry cirrus occur over all latitudes of the tropics, from the equatorial region to the northern and southern edges of the tropics. These behaviors suggest that dry cirrus at low altitudes are decoupled from dry cirrus at high altitudes. We posit that low-altitude dry cirrus are driven by gravity wave activities in the subtropics, which are waves' temperature perturbations in the troposphere. Gravity wave activities are expected to be more prevalent in the winter months than the summer months in each hemisphere.

, consistently with the seasonal pattern of the IWP of dry cirrus clouds in Fig. 8(d).

5 Summary

Based on the monthly anomalies of the SPH and temperature in cloudy air relative to cloud-free airall-sky condition, we have separated the population of tropical cirrus clouds detected by CALIPSO into those of convective origin (convective cirrus) and those of non-convective origins (non-convective cirrus). Convective cirrus occur in moist conditions and include (i) those that form from the freezing of liquid cloud droplets in convective updrafts, (ii) those that form by in situ ice nucleation from the vapor phase due to the adiabatic or diabatic cooling at the top of deep convection, and (iii) those that form by in situ ice nucleation in the moist air of the convective outflows. Non-convective moist cirrus and dry cirrus. We define moist cirrus as those occurring in air that contains more moisture than usual, while dry cirrus occur in dry conditions and form by in situ ice nucleation in response to negative temperature anomaliesair that is colder and contains less moisture than usual.

Convective cirrus tend to occur Moist cirrus are on average located at lower altitudes than non-convective dry cirrus. The level of maximum convective moist cirrus occurrence is at near 14 km, i.e., the bottom of the TTL. In comparison, non-convective dry cirrus obtain their maximum frequency of occurrence at 16 km. The ratio of the number of convective moist cirrus to the number of non-convective cirrus is about 3dry cirrus is on the order of 2:1 over all altitudes of the tropical atmosphere, 3:1

below 14 km, 1:1 above 14 km, and 1:3 above the CPT. The majority of ~~non-convective~~ dry cirrus are located above 14 km, but there are also ~~non-convective~~ dry cirrus below 14 km. ~~Non-convective~~ Dry cirrus at high altitudes occur ~~near the equator, while non-convective~~ in the deep tropics, while dry cirrus at low altitudes occur ~~at higher latitudes at~~ all over the tropics, from the equatorial region to the northern and southern edges of the tropics.

The seasonal cycle of ~~convective~~ moist cirrus is consistent with that of tropical convection, while the seasonal cycle of ~~non-convective~~ dry cirrus above 14 km is consistent with that of the CPT. There are two maxima in the frequency of occurrence of ~~convective~~ moist cirrus, one at around ~~10 °S~~ 11 °S–12 °S in the austral summer, and the other at around ~~10 °N~~ 11 °N–12 °N in the boreal summer. In contrast, ~~non-convective~~ dry cirrus above 14 km occur most frequently ~~near the equator~~ in the deep tropics in the boreal winter when the CPT is coldest. ~~Non-convective~~ Dry cirrus below 14 km occur most frequently in the winter months of each hemisphere whence wave activities are strongest. ~~Overall there are more convective cirrus in the NH than the SH but more non-convective cirrus in the SH than the NH~~These results suggest that the monthly occurrence of moist cirrus, high-altitude dry cirrus, and low-altitude dry cirrus are driven by different process mechanisms: (i) the occurrence of moist cirrus is driven by the moistening effect of convection, (ii) the occurrence of high-altitude dry cirrus is driven by the adiabatic cooling associated with the BDC as well as wave activities in the TTL and lower stratosphere, and (iii) the occurrence of low-altitude dry cirrus is driven by wave activities in the troposphere.

The IWC in both ~~convective and non-convective~~ moist and dry cirrus increases with increasing temperature (decreasing altitude). Thus, ~~non-convective~~ dry cirrus—which on average occur at lower temperatures (higher altitudes)—tend to have lower IWCs than ~~convective~~ moist cirrus. However, at a given altitude, the IWCs in ~~convective and non-convective~~ moist and dry cirrus are comparable to one another~~(at least in the same order of magnitude)~~. Fresh outflow convective anvil cirrus may have much larger IWCs, but subsequent processes during their life cycles such as ice sedimentation and sublimation, and cloud horizontal spreading ~~and ice sublimation~~ can decrease the IWCs by several orders of magnitude as shown in previous ~~modeling~~ studies [*Boehm et* al., 1999; *Luo and Rossow*, 2004; *Dinh et al.*, 2010, 2012~~, 2014~~; *Gehlot and Quaas*, 2012; *Dinh et* al., 2014; *Jensen et* al., 2018; *Gasparini et* al., 2021].

The method proposed here to study cirrus clouds can be applied in model development to improve the representation of cirrus clouds in numerical simulations. We have demonstrated that the spatiotemporal distribution of cirrus clouds is governed by the SPH, temperature, and their variations. Therefore, models would need to accurately represent the SPH, temperature, and their variances in order to accurately simulate the distribution of cirrus clouds. It would be useful to compare between observations and numerical simulations in terms of the frequency and magnitude of the moisture and temperature anomalies and how they affect the occurrence of cirrus clouds. Such a comparison would reveal the specific strategies on how to adjust the model parameterization schemes (e.g., the convection scheme, the gravity wave drag scheme, and/or the microphysics scheme) to improve the representation of cirrus clouds in models.

Author contributions. Qin Huang carried out the analysis of the data. Both Qin Huang and Tra Dinh contributed to writing the manuscript.

Competing interests. No competing interests are present.

Acknowledgements. We thank D. Winker for the discussions at the AGU Fall Meeting in 2019, which motivate this work. We thank Blaž Gasparini and an anonymous reviewer for their feedback and comments which help improving the manuscript.

References

Adler, R. F., Huffman, G. J., Chang, A., Ferraro, R., Xie, P.-P., Janowiak, J., Rudolf, B., Schneider, U., Curtis, S., Bolvin, D., Gruber, A., Susskind, J., Arkin, P., and Nelkin, E.: The Version-2 Global Precipitation Climatology Project (GPCP) Monthly Precipitation Analysis (1979–Present), J. Hydrol., 4, 1147–1167, https://doi.org/10.1175/1525-7541(2003)004<1147:TVGPCP>2.0.CO;2, 2003.

Boehm, M. T. and Verlinde, J.: Stratospheric influence on upper tropospheric tropical cirrus, Geophys. Res. Lett., 27, 3209–3212, https://doi.org/10.1029/2000GL011678, 2000.

Boehm, M. T., Verlinde, J., and Ackerman, T. P.: On the maintenance of high tropical cirrus, J. Geophys. Res., 104, 24 423–24 433, https://doi.org/10.1029/1999JD900798, 1999.

Boucher, O., Randall, D., Artaxo, P., Bretherton, C., Feingold, G., Forster, P., Kerminen, V.-M., Kondo, Y., Liao, H., Lohmann, U., Rasch, P., Satheesh, S. K., Sherwood, S., Stevens, B., and Zhang, X. Y.: Clouds and Aerosols, in: Climate Change 2013: The Physical Science Basis. Contribution of Working Group I to the Fifth Assessment Report of the Intergovernmental Panel on Climate Change, edited by Stocker, T. F., Qin, D., Plattner, G.-K., Tignor, M., Allen, S. K., Boschung, J., Nauels, A., Xia, Y., Bex, V., and Midgley, P. M., pp. 571–658, Cambridge University Press, Cambridge, United Kingdom and New York, NY, USA, https://doi.org/10.1017/CBO9781107415324.016, 2013.

Cairo, F., De Muro, M., Snels, M., Di Liberto, L., Bucci, S., Legras, B., Kottayil, A., Scoccione, A., and Ghisu, S.: Lidar observations of cirrus clouds in Palau (7°33′ N, 134°48′ E), Atmos. Chem. Phys., 21, 7947–7961, https://doi.org/10.5194/acp-21-7947-2021, 2021.

Corti, T., Luo, B. P., Peter, T., Vömel, H., and Fu, Q.: Mean radiative energy balance and vertical mass fluxes in the equatorial upper troposphere and lower stratosphere, Geophys. Res. Lett., 32, L06 802, https://doi.org/10.1029/2004GL021889, 2005.

Corti, T., Luo, B. P., Fu, Q., Vömel, H., and Peter, T.: The impact of cirrus clouds on tropical troposphere-to-stratosphere transport, Atmos. Chem. Phys., 6, 2539–2547, https://doi.org/10.5194/acp-6-2539-2006, 2006.

Corti, T., Luo, B. P., de Reus, M., Brunner, D., Cairo, F., Mahoney, M. J., Martucci, G., Matthey, R., Mitev, V., dos Santos, F. H., Schiller, C., Shur, G., Sitnikov, N. M., Spelten, N., Vössing, H. J., Borrmann, S., and Peter, T.: Unprecedented evidence for overshooting convection hydrating the tropical stratosphere, Geophys. Res. Lett., 35, https://doi.org/10.1029/2008GL033641, 2008.

Das, S. K., Chiang, C.-W., and Nee, J.-B.: Influence of tropical easterly jet on upper tropical cirrus: An observational study from CALIPSO, Aura-MLS, and NCEP/NCAR data, J. Geophys. Res. Atmos., 116, https://doi.org/10.1029/2011JD015923, 2011.

Dessler, A. E., Palm, S. P., Hart, W. D., and Spinhirne, J. D.: Tropopause-level thin cirrus coverage revealed by ICESat/Geoscience Laser Altimeter System, J. Geophys. Res., 111, D08 203, https://doi.org/10.1029/2005JD006586, 2006.

Dessler, A. E., Schoeberl, M. R., Wang, T., Davis, S. M., and Rosenlof, K. H.: Stratospheric water vapor feedback, P. Natl. Acad. Sci., 110, 18 087–91, https://doi.org/10.1073/pnas.1310344110, 2013.

Dinh, T. and Fueglistaler, S.: Cirrus, Transport, and Mixing in the Tropical Upper Troposphere, J. Atmos. Sci., 71, 1339–1352, https://doi.org/10.1175/JAS-D-13-0147.1, 2014a.

Dinh, T. and Fueglistaler, S.: Microphysical, radiative and dynamical impacts of thin cirrus clouds on humidity in the tropical tropopause layer and stratosphere, Geophys. Res. Lett., 41, 6949–6955, https://doi.org/10.1002/2014GL061289, 2014b.

Dinh, T., Durran, D. R., and Ackerman, T.: Maintenance of tropical tropopause layer cirrus, J. Geophys. Res., 115, D02 104, https://doi.org/10.1029/2009JD012735, 2010.

Dinh, T., Durran, D. R., and Ackerman, T.: Cirrus and water vapor transport in the tropical tropopause layer – Part 1: A specific case modeling study, Atmos. Chem. Phys., 12, 9799–9815, https://doi.org/10.5194/acp-12-9799-2012, 2012.

Dinh, T., Fueglistaler, S., Durran, D., and Ackerman, T.: Cirrus and water vapour transport in the tropical tropopause layer – Part 2: Roles of ice nucleation and sedimentation, cloud dynamics, and moisture conditions, Atmos. Chem. Phys., 14, 12,225–12,236, https://doi.org/10.5194/acp-14-12225-2014, 2014.

Dinh, T., Podglajen, A., Hertzog, A., Legras, B., and Plougonven, R.: Effect of gravity wave temperature fluctuations on homogeneous ice nucleation in the tropical tropopause layer, Atmos. Chem. Phys., 16, 35–46, https://doi.org/10.5194/acp-16-35-2016, 2016.

Folkins, I. and Martin, R. V.: The Vertical Structure of Tropical Convection and Its Impact on the Budgets of Water Vapor and Ozone, J. Atmos. Sci., 62, 1560–1573, https://doi.org/10.1175/JAS3407.1, 2005.

Forster, P. M. d. F. and Shine, K. P.: Assessing the climate impact of trends in stratospheric water vapor, Geophys. Res. Lett., 29, 1086, https://doi.org/10.1029/2001GL013909, 2002.

Fueglistaler, S., Dessler, A. E., Dunkerton, T. J., Folkins, I., Fu, Q., and Mote, P. W.: Tropical tropopause layer, Rev. Geophys., 47, RG1004, https://doi.org/10.1029/2008RG000267, 2009.

Fujiwara, M., Iwasaki, S., Shimizu, A., Inai, Y., Shiotani, M., Hasebe, F., Matsui, I., Sugimoto, N., Okamoto, H., Nishi, N., Hamada, A., Sakazaki, T., and Yoneyama, K.: Cirrus observations in the tropical tropopause layer over the western Pacific, J. Geophys. Res., 114, D09 304, https://doi.org/10.1029/2008JD011040, 2009.

Garrett, T. J., Heymsfield, A. J., McGill, M. J., Ridley, B. A., Baumgardner, D. G., Bui, T. P., and Webster, C. R.: Convective generation of cirrus near the tropopause, J. Geophys. Res. Atmos., 109, https://doi.org/10.1029/2004JD004952, 2004.

Gasparini, B., Blossey, P. N., Hartmann, D. L., Lin, G., and Fan, J.: What Drives the Life Cycle of Tropical Anvil Clouds?, J. Adv. Model. Earth Syst., 11, 2586–2605, https://doi.org/10.1029/2019MS001736, 2019.

Gasparini, B., Rasch, P. J., Hartmann, D. L., Wall, C. J., and Dütsch, M.: A Lagrangian Perspective on Tropical Anvil Cloud Lifecycle in Present and Future Climate, J. Geophys. Res. Atmos., 126, e2020JD033 487, https://doi.org/10.1029/2020JD033487, 2021.

Gehlot, S. and Quaas, J.: Convection–Climate Feedbacks in the ECHAM5 General Circulation Model: Evaluation of Cirrus Cloud Life Cycles with ISCCP Satellite Data from a Lagrangian Trajectory Perspective, J. Climate, 25, 5241–5259, https://doi.org/10.1175/JCLI-D-11-00345.1, 2012.

Gettelman, A., Salby, M. L., and Sassi, F.: Distribution and influence of convection in the tropical tropopause region, J. Geophys. Res., 107, 4080, 2002.

Hartmann, D. L., Holton, J. R., and Fu, Q.: The heat balance of the tropical tropopause, cirrus, and stratospheric dehydration, Geophys. Res. Lett., 28, 1969–1972, https://doi.org/10.1029/2000GL012833, 2001.

Hersbach, H., Bell, B., Berrisford, P., Hirahara, S., Horányi, A., Muñoz-Sabater, J., Nicolas, J., Peubey, C., Radu, R., Schepers, D., Simmons, A., Soci, C., Abdalla, S., Abellan, X., Balsamo, G., Bechtold, P., Biavati, G., Bidlot, J., Bonavita, M., Chiara, G., Dahlgren, P., Dee, D., Diamantakis, M., Dragani, R., Flemming, J., Forbes, R., Fuentes, M., Geer, A., Haimberger, L., Healy, S., Hogan, R. J., Hólm, E., Janisková, M., Keeley, S., Laloyaux, P., Lopez, P., Lupu, C., Radnoti, G., Rosnay, P., Rozum, I., Vamborg, F., Villaume, S., and Thépaut, J.: The ERA5 global reanalysis, Q. J. R. Meteorol. Soc., 146, 1999–2049, https://doi.org/10.1002/qj.3803, 2020.

Heymsfield, A. J., Krämer, M., Luebke, A., Brown, P., Cziczo, D. J., Franklin, C., Lawson, P., Lohmann, U., McFarquhar, G., Ulanowski, Z., and Tricht, K. V.: Cirrus Clouds, Meteor. Mon., 58, 2.1–2.26, https://doi.org/10.1175/amsmonographs-d-16-0010.1, 2017.

Highwood, E. J. and Hoskins, B. J.: The tropical tropopause, Q. J. R. Meteorol. Soc., 124, 1579–1604, https://doi.org/10.1002/qj.49712454911, 1998.

Holton, J. R., Haynes, P. H., McIntyre, M. E., Douglass, A. R., Rood, R. B., and Pfister, L.: Stratosphere-troposphere exchange, Rev. Geophys., 33, 403–439, https://doi.org/10.1029/95RG02097, 1995.

Hong, Y. and Liu, G.: The Characteristics of Ice Cloud Properties Derived from CloudSat and CALIPSO Measurements, J. Climate, 28, 3880–3901, https://doi.org/10.1175/JCLI-D-14-00666.1, 2015.

Immler, F., Krüger, K., Fujiwara, M., Verver, G., Rex, M., and Schrems, O.: Correlation between equatorial Kelvin waves and the occurrence of extremely thin ice clouds at the tropical tropopause, Atmos. Chem. Phys., 8, 4019–4026, https://doi.org/10.5194/acp-8-4019-2008, 2008.

Jensen, E. J., Pfister, L., Ackerman, A. S., and Tabazadeh, A.: A conceptual model of the dehydration of air due to freeze-drying by optically thin, laminar cirrus rising slowly across the tropical tropopause, J. Geophys. Res., 106, 17 237–17 252, https://doi.org/10.1029/2000JD900649, 2001.

Jensen, E. J., Ackerman, A. S., and Smith, J. A.: Can overshooting convection dehydrate the tropical tropopause layer?, J. Geophys. Res. Atmos., 112, 2–6, https://doi.org/10.1029/2006JD007943, 2007.

Jensen, E. J., van den Heever, S. C., and Grant, L. D.: The Life Cycles of Ice Crystals Detrained From the Tops of Deep Convection, J. Geophys. Res. Atmos., 123, 9624–9634, https://doi.org/10.1029/2018JD028832, 2018.

Jensen, E. J., Pan, L. L., Honomichl, S., Diskin, G. S., Krämer, M., Spelten, N., Günther, G., Hurst, D. F., Fujiwara, M., Vömel, H., Selkirk, H. B., Suzuki, J., Schwartz, M. J., and Smith, J. B.: Assessment of Observational Evidence for Direct Convective Hydration of the Lower Stratosphere, J. Geophys. Res. Atmos., 125, e2020JD032 793, https://doi.org/10.1029/2020JD032793, 2020.

Jucker, M. and Gerber, E. P.: Untangling the Annual Cycle of the Tropical Tropopause Layer with an Idealized Moist Model, J. Climate, 30, 7339–7358, https://doi.org/10.1175/JCLI-D-17-0127.1, 2017.

Kahn, B. H., Liang, C. K., Eldering, A., Gettelman, A., Yue, Q., and Liou, K. N.: Tropical thin cirrus and relative humidity observed by the Atmospheric Infrared Sounder, Atmos. Chem. Phys., 8, 1501–1518, https://doi.org/10.5194/acp-8-1501-2008, 2008.

Kahn, B. H., Gettelman, A., Fetzer, E. J., Eldering, A., and Liang, C. K.: Cloudy and clear-sky relative humidity in the upper troposphere observed by the A-train, J. Geophys. Res., 114, D00H02, https://doi.org/10.1029/2009JD011738, 2009.

Kim, J., Alexander, M. J., Bui, T. P., Dean-Day, J. M., Lawson, R. P., Woods, S., Hlavka, D., Pfister, L., and Jensen, E. J.: Ubiquitous influence of waves on tropical high cirrus clouds, Geophys. Res. Lett., 43, 5895–5901, 2016.

Kim, J., Randel, W. J., and Birner, T.: Convectively Driven Tropopause-Level Cooling and Its Influences on Stratospheric Moisture, J. Geophys. Res. Atmos., 123, 590–606, https://doi.org/10.1002/2017JD027080, 2018.

Krämer, M., Rolf, C., Luebke, A., Afchine, A., Spelten, N., Costa, A., Meyer, J., Zoeger, M., Smith, J., Herman, R. L., et al.: A microphysics guide to cirrus clouds–Part 1: Cirrus types, Atmos. Chem. Phys., 16, 3463–3483, https://doi.org/10.5194/acp-16-3463-2016, 2016.

Krämer, M., Rolf, C., Spelten, N., Afchine, A., Fahey, D., Jensen, E., Khaykin, S., Kuhn, T., Lawson, P., Lykov, A., Pan, L. L., Riese, M., Rollins, A., Stroh, F., Thornberry, T., Wolf, V., Woods, S., Spichtinger, P., Quaas, J., and Sourdeval, O.: A microphysics guide to cirrus–Part 2: Climatologies of clouds and humidity from observations, Atmos. Chem. Phys., 20, 12 569–12 608, https://doi.org/10.5194/acp-20-12569-2020, 2020.

Li, J.-L. F., Waliser, D. E., Chen, W.-T., Guan, B., Kubar, T., Stephens, G., Ma, H.-Y., Deng, M., Donner, L., Seman, C., and Horowitz, L.: An observationally based evaluation of cloud ice water in CMIP3 and CMIP5 GCMs and contemporary reanalyses using contemporary satellite data, J. Geophys. Res., 117, D16 105, https://doi.org/10.1029/2012JD017640, 2012.

Liao, X. and Rind, D.: Local upper tropospheric/lower stratospheric clear-sky water vapor and tropospheric deep convection, J. Geophys. Res. Atmos., 102, 19 543–19 557, https://doi.org/10.1029/97JD01258, 1997.

Liou, K.-N.: Influence of Cirrus Clouds on Weather and Climate Processes: A Global Perspective, Mon. Wea. Rev., 114, 1167–1199, https://doi.org/10.1175/1520-0493(1986)114<1167:IOCCOW>2.0.CO;2, 1986.

Luo, Z. and Rossow, W. B.: Characterizing Tropical Cirrus Life Cycle, Evolution, and Interaction with Upper-Tropospheric Water Vapor Using Lagrangian Trajectory Analysis of Satellite Observations, J. Climate, 17, 4541–4563, 2004.

Mace, G. G., Deng, M., Soden, B., and Zipser, E.: Association of Tropical Cirrus in the 10–15-km Layer with Deep Convective Sources: An Observational Study Combining Millimeter Radar Data and Satellite-Derived Trajectories, J. Atmos. Sci., 63, 480–503, https://doi.org/10.1175/JAS3627.1, 2006.

Mace, G. G., Zhang, Q., Vaughan, M., Marchand, R., Stephens, G., Trepte, C., and Winker, D.: A description of hydrometeor layer occurrence statistics derived from the first year of merged Cloudsat and CALIPSO data, J. Geophys. Res., 114, D00A26, https://doi.org/10.1029/2007JD009755, 2009.

Massie, S., Gettelman, A., Randel, W., and Baumgardner, D.: Distribution of tropical cirrus in relation to convection, J. Geophys. Res., 107, 4591, https://doi.org/10.1029/2001JD001293, 2002.

Mote, P. W., Rosenlof, K. H., McIntyre, M. E., Carr, E. S., Gille, J. C., Holton, J. R., Kinnersley, J. S., Pumphrey, H. C., Russell, J. M., and Waters, J. W.: An atmospheric tape recorder: The imprint of tropical tropopause temperatures on stratospheric water vapor, J. Geophys. Res., 101, 3989–4006, https://doi.org/10.1029/95JD03422, 1996.

Murphy, D. M. and Koop, T.: Review of the vapour pressures of ice and supercooled water for atmospheric applications, Q. J. R. Meteorol. Soc., 131, 1539–1565, https://doi.org/10.1256/qj.04.94, 2005.

NASA Langley Atmospheric Science Data Center: CALIPSO Lidar Level 3 Ice Cloud Data, Standard V1-00, https://doi.org/10.5067/CALIOP/CALIPSO/L3_ICE_CLOUD-STANDARD-V1-00, 2018.

Nee, J.-B. and Lu, C.-Y.: Seasonal migration of cirrus clouds by using CALIOP observations, Meteorol. Atmos. Phys., 133, 579–587, https://doi.org/10.1007/s00703-020-00769-8, 2021.

Pfister, L., Selkirk, H. B., Jensen, E. J., Schoeberl, M. R., Toon, O. B., Browell, E. V., Grant, W. B., Gary, B., Mahoney, M. J., Bui, T. V., and Hintsa, E.: Aircraft observations of thin cirrus clouds near the tropical tropopause, J. Geophys. Res. Atmos., 106, 9765–9786, https://doi.org/10.1029/2000JD900648, 2001.

Plumb, R. A. and Eluszkiewicz, J.: The Brewer–Dobson Circulation: Dynamics of the Tropical Upwelling, J. Atmos. Sci., 56, 868–890, https://doi.org/10.1175/1520-0469(1999)056<0868:TBDCDO>2.0.CO;2, 1999.

Reinares Martínez, I., Evan, S., Wienhold, F. G., Brioude, J., Jensen, E. J., Thornberry, T. D., Héron, D., Verreyken, B., Körner, S., Vömel, H., Metzger, J.-M., and Posny, F.: Unprecedented Observations of a Nascent In Situ Cirrus in the Tropical Tropopause Layer, Geophys. Res. Lett., 48, e2020GL090 936, https://doi.org/10.1029/2020GL090936, 2021.

Robinson, F. J. and Sherwood, S. C.: Modeling the Impact of Convective Entrainment on the Tropical Tropopause, J. Atmos. Sci., 63, 1013–1027, https://doi.org/10.1175/JAS3673.1, 2006.

Salathé, E. P. and Hartmann, D. L.: A Trajectory Analysis of Tropical Upper-Tropospheric Moisture and Convection, J. Climate, 10, 2533–2547, https://doi.org/10.1175/1520-0442(1997)010<2533:ATAOTU>2.0.CO;2, 1997.

Sandor, B. J., Jensen, E. J., Stone, E. M., Read, W. G., Waters, J. W., and Mergenthaler, J. L.: Upper tropospheric humidity and thin cirrus, Geophys. Res. Lett., 27, 2645–2648, https://doi.org/10.1029/1999GL011194, 2000.

Sassen, K., Wang, Z., and Liu, D.: Global distribution of cirrus clouds from CloudSat/Cloud-Aerosol Lidar and Infrared Pathfinder Satellite Observations (CALIPSO) measurements, J. Geophys. Res., 113, 1–12, https://doi.org/10.1029/2008JD009972, 2008.

Sassi, F., Salby, M., and Read, W. G.: Relationship between upper tropospheric humidity and deep convection, J. Geophys. Res. Atmos., 106, 17 133–17 146, https://doi.org/10.1029/2001JD900121, 2001.

Schiller, C., Krämer, M., Afchine, A., Spelten, N., and Sitnikov, N.: Ice water content of Arctic, midlatitude, and tropical cirrus, J. Geophys. Res., 113, 1–12, https://doi.org/10.1029/2008JD010342, 2008.

Schiller, C., Grooß, J. U., Konopka, P., Plöger, F., Silva dos Santos, F. H., and Spelten, N.: Hydration and dehydration at the tropical tropopause, Atmos. Chem. Phys., 9, 9647–9660, https://doi.org/10.5194/acp-9-9647-2009, 2009.

Schoeberl, M. R., Jensen, E. J., Pfister, L., Ueyama, R., Avery, M., and Dessler, A. E.: Convective Hydration of the Upper Troposphere and Lower Stratosphere, J. Geophys. Res. Atmos., 123, 4583–4593, https://doi.org/10.1029/2018JD028286, 2018.

Sherwood, S. C., Horinouchi, T., and Zeleznik, H. A.: Convective Impact on Temperatures Observed near the Tropical Tropopause, J. Atmos. Sci., 60, 1847–1856, https://doi.org/10.1175/1520-0469(2003)060<1847:CIOTON>2.0.CO;2, 2003.

Sherwood, S. C., Ingram, W., Tsushima, Y., Satoh, M., Roberts, M., Vidale, P. L., and O'Gorman, P. A.: Relative humidity changes in a warmer climate, J. Geophys. Res., 115, D09 104, https://doi.org/10.1029/2009JD012585, 2010.

Soden, B. J. and Fu, R.: A Satellite Analysis of Deep Convection, Upper-Tropospheric Humidity, and the Greenhouse Effect, J. Climate, 8, 2333–2351, https://doi.org/10.1175/1520-0442(1995)008<2333:ASAODC>2.0.CO;2, 1995.

Sohn, B.-J., Schmetz, J., and Chung, E.-S.: Moistening processes in the tropical upper troposphere observed from Meteosat measurements, J. Geophys. Res. Atmos., 113, https://doi.org/10.1029/2007JD009527, 2008.

Solomon, S., Rosenlof, K. H., Portmann, R. W., Daniel, J. S., Davis, S. M., Sanford, T. J., and Plattner, G.-K.: Contributions of stratospheric water vapor to decadal changes in the rate of global warming, Science, 327, 1219–1223, https://doi.org/10.1126/science.1182488, 2010.

Spang, R., Eidmann, G., Riese, M., Offermann, D., and Preusse, P.: CRISTA observations of cirrus clouds around the tropopause, J. Geophys. Res., 107, 1–18, https://doi.org/10.1029/2001JD000698, 2002.

Takahashi, H. and Luo, Z.: Where is the level of neutral buoyancy for deep convection?, Geophys. Res. Lett., 39, https://doi.org/10.1029/2012GL052638, 2012.

Taylor, J. R., Randel, W. J., and Jensen, E. J.: Cirrus cloud-temperature interactions in the tropical tropopause layer: a case study, Atmos. Chem. Phys., 11, 10 085–10 095, https://doi.org/10.5194/acp-11-10085-2011, 2011.

Tseng, H.-H. and Fu, Q.: Tropical tropopause layer cirrus and its relation to tropopause, J. Quant. Spectrosc. Ra., 188, 118–131, https://doi.org/10.1016/j.jqsrt.2016.05.029, 2017.

Ueyama, R., Jensen, E. J., Pfister, L., and Kim, J.-E.: Dynamical, convective, and microphysical control on wintertime distributions of water vapor and clouds in the tropical tropopause layer, J. Geophys. Res. Atmos., 120, 10,483–10,500, https://doi.org/10.1002/2015JD023318, 2015.

Ueyama, R., Jensen, E. J., and Pfister, L.: Convective Influence on the Humidity and Clouds in the Tropical Tropopause Layer During Boreal Summer, J. Geophys. Res. Atmos., 123, 7576–7593, https://doi.org/10.1029/2018JD028674, 2018.

Virts, K. S. and Wallace, J. M.: Annual, interannual, and intraseasonal variability of tropical tropopause transition layer cirrus, J. Atmos. Sci., 67, 3097–3112, https://doi.org/10.1175/2010JAS3413.1, 2010.

Virts, K. S., Wallace, J. M., Fu, Q., and Ackerman, T. P.: Tropical tropopause transition layer cirrus as represented by CALIPSO lidar observations, J. Atmos. Sci., 67, 3113–3129, https://doi.org/10.1175/2010JAS3412.1, 2010.

Wang, P.-H., Minnis, P., McCormick, M. P., Kent, G. S., and Skeens, K. M.: A 6-year climatology of cloud occurrence frequency from Stratospheric Aerosol and Gas Experiment II observations (1985–1990), J. Geophys. Res., 101, 29 407–29 429, https://doi.org/10.1029/96JD01780, 1996.

Wang, T. and Dessler, A. E.: Analysis of cirrus in the tropical tropopause layer from CALIPSO and MLS data: A water perspective, J. Geophys. Res., 117, D04 211, https://doi.org/10.1029/2011JD016442, 2012.

Waugh, D. W. and Polvani, L. M.: Climatology of intrusions into the tropical upper troposphere, Geophys. Res. Lett., 27, 3857–3860, https://doi.org/10.1029/2000GL012250, 2000.

Winker, D. M., Hunt, W. H., and McGill, M. J.: Initial performance assessment of CALIOP, Geophys. Res. Lett., 34, https://doi.org/10.1029/2007GL030135, 2007.

Winker, D. M., Pelon, J., Coakley, J. A., Ackerman, S. A., Charlson, R. J., Colarco, P. R., Flamant, P., Fu, Q., Hoff, R. M., Kittaka, C., Kubar, T. L., Treut, H. L., Mccormick, M. P., Mégie, G., Poole, L., Powell, K., Trepte, C., Vaughan, M. A., and Wielicki, B. A.: The CALIPSO Mission: A Global 3D View of Aerosols and Clouds, Bull. Am. Meteorol. Soc., 91, 1211–1230, https://doi.org/10.1175/2010BAMS3009.1, 2010.

Wright, J. S., Fu, R., and Heymsfield, A. J.: A statistical analysis of the influence of deep convection on water vapor variability in the tropical upper troposphere, Atmos. Chem. Phys., 9, 5847–5864, https://doi.org/10.5194/acp-9-5847-2009, 2009.

Xie, S.-P.: The Shape of Continents, Air-Sea Interaction, and the Rising Branch of the Hadley Circulation, in: The Hadley Circulation: Present, Past and Future, edited by Diaz, H. F. and Bradley, R. S., Advances in Global Change Research, pp. 121–152, Springer Netherlands, Dordrecht, https://doi.org/10.1007/978-1-4020-2944-8_5, 2004.

Yulaeva, E., Holton, J. R., and Wallace, J. M.: On the Cause of the Annual Cycle in Tropical Lower-Stratospheric Temperatures, J. Atmos. Sci., 51, 169–174, https://doi.org/10.1175/1520-0469(1994)051<0169:OTCOTA>2.0.CO;2, 1994.

Zhang, S. D., Yi, F., Huang, C. M., and Zhou, Q.: Latitudinal and seasonal variations of lower atmospheric inertial gravity wave energy revealed by US radiosonde data, Ann. Geophys., 28, 1065–1074, https://doi.org/10.5194/angeo-28-1065-2010, 2010.